Title
Revealing the natural complexity of topographic change processes through repeat surveys and decision-tree classification

Authors
Wyrick, Joshua R
Pasternack, Gregory B

Publication Date
2015-10-01

DOI
10.1002/esp.3854

Peer reviewed

Title: Revealing the natural complexity of topographic change processes through repeat surveys and decision-tree classification

Short title: Decision tree classification of topographic change processes

Authors: Joshua R. Wyrick*[a], Gregory B. Pasternack[b]

[a] Lafayette College, 740 High Street, Easton, PA, 18042

[b] University of California, Davis, One Shields Drive, Davis, CA, 95616

* Corresponding author. Tel.: + 1 610-330-5735; E-mail: wyrickj@lafayette.edu; Fax: + 1 610-330-5059

Keywords: topographic change; DEM differencing; river morphology; regulated rivers; geomorphic change

Abstract

Topographic change processes (TCPs) are the mechanisms by which a landscape is interpreted to be experiencing landform deformation, and are defined by the specific actions occurring within a contiguous, localized region that cause sediment to be either deposited or eroded. Past topographic change studies have mostly been focused at the site scale. The goal of this study was to identify and delineate spatially explicit TCP types across the valley width in a 34-km long cobble-gravel river at the scale of $1/10^{th}$ of the bankfull channel width over a period of 7-9 years. To accomplish this, a new procedure was developed that analyzes spatial patterns of topographic change evident from differencing two raster digital elevation models and accounting for sources of uncertainty, then identifying and classifying those changes using a decision tree framework that invokes the locations of those changes as they relate to the locations of specific geographic characteristics. Once mapped, TCP polygons were analyzed for areal patterns and volumetric rates of change. Results showed that 19 unique TCP types occurred and that they have organized but complex spatial patterns. Within this study segment, overbank storage processes occurred over the most area and displaced the most net volume of sediment, while cohesive bank retreat created the largest net change in topographic elevations. Analyses of the TCPs reveal that the regulated lower Yuba River (LYR) is not experiencing the expected combination of channel incision and floodplain deposition commonly reported below dams. Instead, the LYR is a dynamic valley that is still adjusting valley-wide to the upstream dam with a diverse suite of processes that cause the channel and floodplains to scour and fill in concert.

Introduction

Quantification of changes in river morphology provides a means for monitoring rates and directions of landform change as well as analyzing fluvial sediment budgets relevant to landscape evolution, river engineering, and ecosystem services. Although geomorphologists have long recognized that topographic change is spatially complex on the basis of qualitative description (e.g. Goff and Ashmore, 1993; Lane *et al.*, 1994), time, cost, and insufficient technology historically constrained topographic change studies to cross-section based analyses in which the same lines across a river were repeatedly surveyed over years and changes were assessed by plotting the elevational profiles together on one figure (e.g. Leopold *et al*., 1964; Warburton *et al*., 1993). Ferguson *et al*. (1992) explained a standard procedure for computing a reach-scale volumetric sediment flux using cross-sectional data by computing erosion and deposition volumes independently through a local averaging and spatial summing procedure. Alternatively, individual processes such as bank retreat can be identified and then a small sampling of local topographic changes would be extrapolated (usually through planimetric analysis of aerial photographs and/or maps) to estimate reach, segment, or catchment scale fluxes (e.g. Hadley and Schumm, 1961).

Today, large, detailed topographic datasets are increasingly available and geomorphologists are rapidly developing commensurate methods for analyzing geomorphology with respect to its natural spatial complexity. A pioneering study in this new spatially explicit paradigm for quantitative fluvial geomorphology was the work of Lane *et al*. (1994), and the study herein builds on that legacy by developing an algorithm for identifying and mapping areas exhibiting spatially coherent and spatially distributed topographic change processes using a digital elevation model (DEM) of differences and a decision tree. When applied to a dynamic cobble-gravel river, the results show a remarkable assemblage of processes that offer a novel perspective on how rivers change through time.

DEMs and DEM differencing

In the last decade, segment-scale (~10^3–10^4 channel widths), meter-resolution mapping techniques for subaerial and subaqueous topography have come into existence, become cheaper, and are more readily adopted (Hilldale and Raff, 2008; Costa *et al*., 2009), with further improvements occurring very rapidly (Javernick *et al*., 2014). Theories and methods for development and use of DEMs from such data have existed for a long time (Moore *et al*., 1991) and continue to progress (Bishop *et al*., 2012; Wilson, 2012). As a result, spatially explicit geomorphic and ecological methods applying DEMs are being developed to yield studies of physical habitat structure (Hall *et al*., 2009; Pasternack, 2011), sediment dynamics (Fuller and Basher, 2013), river restoration procedures and outcomes (Merz *et al*., 2006; Sawyer *et al*., 2009), rates of eco-geomorphic changes (Grabowski *et al*., 2014), and channel responses to fluvial drivers (Wheaton *et al*., 2010b; Wheaton *et al*., 2013) that are accurate, detailed, and useful for river science and management.

In terms of fluvial sediment budgeting for the study presented herein, DEMs collected at different times are compared by subtracting, or “differencing”, one from another (e.g. Lane *et al*., 1994; Brasington *et al*., 2000). Compared to cross-sectional analyses, DEM differencing provides a better estimate of the magnitude of volumetric changes (Fuller *et al*., 2003), allows for a reliable estimate of uncertainty of the estimated changes (Wheaton *et al*., 2010a), aggregates results at different scales above the grid-scale resolution accounting for statistical variability, and explicitly identifies spatial patterns of scour and fill at the grid-scale resolution. The results provide a better understanding of spatial patterns and magnitudes of topographic change in rivers, which in turn means there is an opportunity to answer such questions in geomorphology that consider the natural complexity inherent in a three dimensional world (Wheaton *et al*., 2013). Nevertheless, there remain important methodological gaps and uncertainties limiting wider adoption. The study herein analyzes segment-scale, meter-resolution DEM differences to identify the types of processes that occurred to create the current morphology of a 34-km regulated river system.

Topographic change processes

Topographic change processes (TCP) are the mechanisms by which a landscape is interpreted by trained geomorphologists to be experiencing landform deformation. The term *topographic change process* is used herein, instead of the similar *geomorphic change process*, because it is more explicit and descriptive of what is happening – a *process* that *changes* the *topography*. Scientific convention holds that topography refers to the elevation of a surface. Therefore, change to elevation between two moments in time (i.e., one epoch) is properly termed *topographic change*. If one were to look at how a topographic change process were then to change between two epochs (i.e., through four moments in time) if it did not remain constant, then we propose to use the term *geomorphic change processes* as a second order mechanism describing changes to topographic change process through time, as opposed to terming this topographic change change. Thus, topographic change and geomorphic change are not synonymous. This therefore is the proposed lexicon for beginning with a single topography and taking the first and second derivatives of it through time. A TCP is defined by the specific action occurring within a contiguous, localized region that causes sediment to be either deposited or eroded. In the fluvial context, a TCP is usually a hydraulic mechanism that affects the underlying and surrounding morphology (e.g. lateral migration, bed incision, bar deposition, etc.) or a water-influenced mass wasting mechanism (Barker *et al*., 1997; Darby *et al*., 2007), including riverbank freeze-thaw (Yumoto *et al*., 2006). There is a feedback loop between channel morphology and TCPs, such that a TCP that occurs to create a particular landform could be substantively altered by the presence of that new landform, thus changing the type of TCP that occurs in that region, which could be described as a geomorphic change process.

Previously, identification and/or spatial delineation of TCPs have generally been focused on small-scale studies, such that TCPs have usually been discussed singularly in response to a localized scour/fill process. At all spatial scales, there is an increasing trend to utilize dense repeat survey data to characterize DEMs of differences (DoDs). However, there is a distinct gap in the literature for combining segment-scale DoDs with expert-based assessment of change processes to create a large-scale TCP map. Wheaton *et al*. (2013) applied a detailed assessment of change processes to a 1-km long reach on a gravel-bed river. Through their multiple DoDs, they were able to identify which specific braiding mechanisms were the most responsible for changes in sediment volumes. Interpreting changes in river topography in terms of specific processes remains an important task for geomorphologists, but today detailed, expansive data and model outputs can be utilized to achieve that goal with more resolution and objectivity, and for larger segments of rivers.

Some topographic change mechanisms are well studied, such as the lateral accretion that occurs as sediment deposits in recirculation zones on the inside bend of a channel meander that creates an emergent bar (e.g. Rubin *et al*., 1990). Other mechanisms may be well documented, but the triggers for their creation are poorly understood, such as for avulsions (e.g. Slingerland and Smith, 1998). Studies that identify a variety of mechanisms responsible for multiple topographic change processes over a long river segment are rare, however.

The ability to delineate specific change processes over multiple scales is important for geomorphologists. The understanding of how valley sediments are consumed and rejuvenated provides insight into the evolution of the channel and landscape morphology. The connectivity between the channel and overbank regions can be strengthened or weakened based on what change processes are allowed to occur. For example, floodplains are usually assumed to form through lateral accretion processes as the channel migrates, causing bars to emerge which eventually become subsumed into the floodplains (e.g. Allen, 1965). However, if channel meandering is hindered, then floodplains will tend to form through vertical accretion processes. If those processes are paired with incision in the non-meandering channel, then a disconnect can arise between the channel and its floodplain. In natural streams, there is an array of processes that lead to floodplain formation, usually striking some balance between lateral and vertical processes (Nanson, 1986). Mid-channel islands are another common river feature that are known to form and scour away by a variety of mechanisms (Wyrick and Klingeman, 2011), which can separate from or join to the floodplains depending on which mechanisms occur. Specific processes that allow for the growth or elimination of fluvial islands are important for maintaining a natural change regime in rivers (e.g. Gurnell and Petts, 2002).

The methodology for delineating TCPs presented herein removes field-observer bias and creates a repeatable approach for identifying and mapping a wide range of TCP types for any spatial scale.

Study Objectives

In light of these concepts, the overall goal of this study was to identify and delineate the mechanisms of topographic change in a dynamic lowland cobble-gravel river, considering 1/10th-width-scale resolution for a long river segment. In this study, we developed an algorithm for identifying and mapping areas exhibiting spatially coherent and spatially distributed topographic change process using a digital elevation model (DEM) of differences and a decision tree. We then applied the method to a 34-km regulated alluvial river segment to revisit the classic question of whether topographic change downstream of a sediment-barrier dam several decades after construction would be dominated by in-channel downcutting and floodplain fill processes, or if other processes would be equally or more important. The specific objectives addressed herein were to (i) devise a methodology for automatic and transparent delineation of TCP types; (ii) determine which TCP types were present in the study site during the 1999-2008 epoch and in what abundances; (iii) assess how much sediment was displaced by each TCP type within the segment, and (iv) use these results to conceptualize the morphologic response of a regulated river 67 years after dam installation.

Because this study is forensic, not predictive, the exact physical hydraulics that caused each change mechanism were not investigated. Instead, the results rely on previously published literature from the study segment and from other rivers that examine and explain these triggers as the basis for our identification and classification of the processes. In addition to aiding the interpretation of the growing number of DEM differencing field studies, the new methods presented herein could also be applied to predictive morphodynamic models (e.g. Nicholas, 2013) to better characterize their outputs and understand how well they represent real systems.

Study Site

Yuba watershed

The 3480 km^2 Yuba River is a tributary in the Sacramento River basin flowing from the western slopes of the Sierra Nevada to the confluence with the Feather River at Marysville (Figure 1). The montane-Mediterranean climate is characterized by cool, wet winters and hot, dry summers (Storer *et al*., 2004). Almost all precipitation occurs from October through April, with a temperature dependent snowline. Snow pack accumulates through the winter at high elevations. Heavy flooding can occur in the winter when weather systems driven by the Pacific Ocean El Nino Southern Oscillation produce warm rain-on-snow events. Spring runoff is dominated by snowmelt during April-June as temperatures warm. Dry conditions prevail May-September with occasional convective thunderstorms at high elevations. Annual precipitation ranges from > 1500 mm for the Sierra Nevada to ~ 500 mm near the mouth (Curtis *et al*., 2005).

Lower Yuba River segment

The ~ 37 km long section between the Englebright Dam and the Feather River confluence is termed the Lower Yuba River (LYR). It exhibits a straight to slightly meandering planform geometry, little entrenchment, a cobble-gravel bed, an average channel slope of 0.16%, and an average wetted baseflow width of 59.4 m (Wyrick and Pasternack, 2012). Even though Englebright Dam blocks bedload, the LYR remains a wandering gravel-bed river with a valley-wide active zone due to the cobble-gravel-rich hydraulic-mining deposits (James *et al*., 2009; White *et al*., 2010). The segment-scale mean substrate diameter is 97 mm (i.e. small cobble); however, the mean substrate size decreases in the downstream direction, from 298 mm (boulder) near Englebright Dam to 40 mm (medium gravel/small cobble) near the mouth. Applying the reach-scale Stream Type classification method (Rosgen, 1996) to the whole LYR segment, the segment is classified as a C3 stream, with some differences for each of eight reaches (Wyrick and Pasternack, 2012). The 8-m Daguerre Point Dam (DPD) was installed ca. 1910 to be a sediment trap about halfway down the LYR (Figure 1). Sediment has since filled in its storage capacity and provides little to no barrier for downstream transport.

Instantaneous stage-discharge has been continuously recorded on the LYR at two USGS gages: Smartsville near Englebright dam (#11418000), and Marysville near the mouth (#11421000). The baseflow discharge (~ 19.8 – 28.3 m^3/s) in the LYR typically occurs during the late fall season that coincides with the Chinook (*Oncorhynchus tshawytscha*) adult spawning period and includes an agricultural withdrawal at DPD of up to 9.9 m^3/s. Wyrick and Pasternack (2012) defined a representative baseflow discharge for research purposes of 24.9 m^3/s above DPD and 15.0 m^3/s downstream of DPD (accounting for an irrigation withdrawal), which is equivalent to ~ 75% daily exceedance probability. The winter flood regime is highly dynamic despite some flow regulation (regulated up to 118.9 m^3/s by Englebright Dam), with a bankfull discharge of ~ 141.6 m^3/s occurring every ~ 1.25 years and the floodplain-filling flow of ~ 597.5 m^3/s occurring every ~ 2.5 years (Wyrick and Pasternack, 2012). Existing LYR literature with more information about the hydrogeomorphic conditions include Pasternack (2008), James *et al*. (2009), Moir and Pasternack (2010), Sawyer *et al*. (2010), and White *et al*. (2010).

The LYR morphology was previously delineated at the ~ 0.1-10 channel-widths scale by identifying specific classes of contiguous landforms, known as morphological units (MUs), that make up the in-channel and overbank areas of the latest-available DEMs (Wyrick and Pasternack, 2012, 2014). Delineation of the MUs was accomplished through a classification of representative base flow depth and velocity rasters that objectively mapped the laterally-explicit in-channel landforms (Wyrick et al., 2014). Bank, floodplain, and outer valley landforms were mapped on an expert basis drawing on many geospatial indicators. In total, 31 distinct MU types were identified and mapped for the full LYR segment, which will become one of the stratification filters for TCP identification. Full descriptions of the MU types and how they were delineated are available in Wyrick and Pasternack (2012).

Survey and DEM data

Two topographic DEM datasets spanning the downstream-most 34 km of the lower Yuba River (i.e. from the onset of Timbuctoo Bend to the mouth, Figure 1) were compared to create a detailed map of the areal and vertical changes in topography. Complete details of the methodology, including spatially explicit uncertainty analysis, as well as a discussion of the implications the DEM differencing maps have on the interpretation of the LYR's landscape evolution are available in Carley *et al*. (2012), but are summarized herein. This study expands upon the earlier work by analyzing the observed spatial patterns of change and classifying those changes by the specific mechanisms that created them.

In 1999, topographic and bathymetric survey data were collected by contractors for the US Army Corp of Engineers to yield a 0.6-m contour map of the LYR. Topographic contours and available point data were combined to produce a 1.5-m resolution DEM using the State Plane California Zone II (feet) coordinate system (NAD83 datum), with the elevations updated to the modern NAVD88 datum. A more recent topographic map of the LYR was produced between 2006 and 2009 through a phased effort as funding and need permitted. Ideally, the entire river would have been surveyed in one brief effort, but resources, available expertise, technology, and variable river conditions necessitated incremental mapping. As it turned out, the survey period between June 2006 and March 2009 was dry with low flows (Figure 2), so it was reasonable to extend mapping over this time frame to meet project constraints. Subsequent analyses that hinge on the duration between topographic maps from section to section of river accounted for different epochs for different areas. Additionally, areas of data gaps within each map and known man-made alterations (e.g. mining pits, dredging spoils, etc.) between mapping efforts were removed from both DEMs before differencing.

The 1999 contour map is a dataset that was provided to the authors as is. For the 2006-2009 surveys, the authors had more control of the survey methods and map production. For these latter DEMs, a comprehensive set of uncertainty analyses was performed to ensure that the multiple surveys used to create the single map were accurate and comparable (for details on the uncertainty analyses, refer to Barker, 2010 and Carley et al., 2012). Ground points on the uneven natural surface were compared between ground-based and boat-based surveys, ground-based and LIDAR surveys, and boat-based and LIDAR surveys. Surveys were also compared at carefully surveyed water surface elevation locations along the water's edge, where surface variability was less. Vertical datums were checked between survey methods. Overall, mean survey differences between methods were within the river's mean grain size (97 mm). A thorough QA/QC report is available in Barker (2010). After all QA/QC analyses were performed and datum adjustments made, a set of TINs were produced for the entire LYR to characterize each survey.

DEM difference map

To overcome the limited point density resulting from digitizing points along contours, Carley *et al*. (2012) applied an artificial point grid to a three-dimensional surface before DEM subtraction. Initially, each topographic surface began as a TIN based on the available source data. A summary workflow for the Carley *et al*. (2012) method using ArcGIS 10.0 is presented in Figure 3. For this system, any differences of ± 0.3 m were considered within the bounds of uncertainty and were labeled as “no detectable change”. The final DoD map represents the net change in topographic elevation over the 7-9 year epoch for each pixel (Supplemental Figure 1). Any ephemeral topographic changes that occurred between the two map dates but did not persist until the second survey cannot be accounted for with this methodology, which is a long-standing constraint on the repeat survey approach (Horne and Patton, 1989).

Methods

Delineation of TCPs

Ideally, there would be some way to continuously observe rivers as they change through time, especially during floods, and then TCPs would be objectively identified and delineated as processes occur. Such an ideal is feasible for numerical morphodynamic models, though not yet implemented. However, neither field geomorphologists nor technologies can see into turbid water in low light or darkness to quantify and map TCPs during floods. Analyses must make do with the surveys that become available as time and money permit. For the LYR, there exists a 1999 survey and a repeat survey in 2006/2008 (different epochs for different reaches of the river). Little morphologic observation occurred during the intervening years, except at the site scale in which riffle-pool maintenance was analyzed in Timbuctoo Bend (Sawyer *et al*., 2010). Therefore, TCP identification must be inferred from the two survey datasets, along with expert knowledge on how a particular process would affect the morphology. Wheaton *et al*. (2013) used a manual, expert-based procedure to interpret DoD rasters and draw polygonal objects for each individual, spatially coherent area where a TCP occurred. In this study, we took a different approach in which we used expert judgment to produce a decision tree for how a DoD should be delineated, but then allowed that algorithm to objectively map TCP polygons. A summary workflow for this method is presented in Figure 4, and expanded upon in the following paragraphs.

Before any definitions or nomenclature of specific TCPs were applied to the LYR, each pixel within the DoD map was segregated and catalogued based on geographic characteristics: whether net scour, fill, or no change occurred during the survey epochs; its spatial location to the wetted channels for both survey end dates; and the physical valley characteristics of each pixel (i.e. morphological unit endform, vegetation presence, sediment size, etc.).

For the first step for TCP delineation, DoD raster pixels were reclassified into either scour, fill, or “no detectable change” in light of the aggressive 95% confidence thresholding used in the spatially explicit uncertainty analysis (Carley *et al*., 2012). Once classified, adjoining cells of the same class were merged into object-oriented polygons.

For the second step, the LYR corridor was segregated into four distinct regions based on the wetted channel boundaries in 1999, 2006 (Timbuctoo Bend reach only), and 2008 (the rest of the alluvial LYR). Ideally this would be done using objectively delineated bankfull channel wetted area maps for each DEM. It is rare to have repeat aerial photos taken at nearly the same discharge many years apart, so an approach was needed to obtain and analyze wetted channels at similar flows. One way would be to reconstruct planform channel regions for each year at the same discharge using two-dimensional hydrodynamic (2D) models (Pasternack, 2011). In this case that was infeasible, because there were enough DEM data gaps in key locations of the 1999 map to inhibit 2D modeling of the river segment. Instead, the approach taken was to use the imagery from the initial year when flow was relatively close to bankfull discharge and then simulate that flow for the later years to obtain the matching planform channel conditions. Specifically, planform channel regions were hand digitized using greyscale aerial imagery collected by Towill, Inc. on April 14, 1999 when the USGS streamflow record indicates a mean daily discharge of 109 m^3/s (3,860 cfs) at the Smartsville gage. Then, planform channel regions were obtained from a pre-exsiting 2D model simulation of the LYR at a discharge of 113 m^3/s (4,000 cfs), which is the closest discharge simulated to that of the 1999 map (Barker, 2011; Abu-Aly *et al*., 2013; Pasternack *et al*., 2014). The flow difference is just 3.6%, which is too small to matter for the purpose of this study. The wetted channel polygons from 1999 and 2006/2008 were overlain and the valley was then divided into four distinct planform regions: (a) outside both channels – not wetted at either time, (b) inside both channels – wetted for both times, (c) outside of 1999 but inside 2008 – was dry then wetted, and (d) inside 1999 but outside 2008 – was wetted then dry.

The LYR valley has previously been delineated based on several other physical characteristics. These rasters were overlain with the DoD raster to provide additional characterizations for each pixel. A vegetation presence/absence raster (Abu-Aly *et al*., 2014) was used to delineate which deposition processes might have been influenced by vegetation, though this only accounts for the effects of vegetation in vegetation and not how it could affect topographic change upstream and downstream of it. The locations of TCPs were identified with respect to features of the morphological unit map (Wyrick and Pasternack, 2012, 2014), such as islands, floodplains, berms, cutbanks, and high flow channels (i.e. swales and flood runners). Sediment size distribution maps (Jackson *et al*., 2013) and field reconnaissance of cutbanks were used to interpret whether some erosion processes occurred in cohesive or non-cohesive sediments.

All contiguous pixels that exhibited the same set of segregation characteristics were coalesced into a singular polygon. Excluding “no detectable elevation change” (which overrode all segregations), combining all segregation steps yielded 19 distinct possible combinations, ten fill processes and nine scour processes (Table 1a, b). The suite of like polygons thus comprises a specific TCP for the LYR valley. Scientific definitions and nomenclature assigned to each type of process that occurred within the LYR (i.e. each specific combination of identified raster characteristics) were first agreed upon within a collaborative consortium of scientists with expert knowledge of the river. The exact names of the processes may differ between river scientists and within the literature; however, they were chosen so as to clearly and plainly represent each process definition. For example, “downcutting” (Table 1b) is a common term used to describe the vertical (downward) erosion within the persistent main channel. This process utilizes the shear stress of the water column acting on the channel bottom to transport its sediments, and as such does not incorporate any process that may lead to meandering (i.e. bank shear stress, weathering and weakening, or mass wasting). Downcutting is purely a process that leads to net negative elevation change within the channel over a given survey epoch. A couple TCP names (berm fill and berm scour) are likely unique to the LYR, because of 19th century hydraulic mining sedimentation and early to mid 20th century re-processing of that material into tailings berms by dredgers.

A decision tree was created to automatically and objectively categorize the polygons into specific TCPs based on the subjective segregations described above (Figure 5). The decision tree may seem large and complicated at first view, but it rests on a few simple principles and choices that are easily understood and applied. This hierarchical segmentation successively splits the DoD dataset into increasingly homogeneous subsets until terminal TCP types are determined. The process was created with full transparency such that future iterations of TCP mapping in other fluvial systems can be done with simple adjustments to the decision tree that will personalize the method to that system. In contrast, manual TCP delineation is more opaque and difficult to systematically amend if the underlying TCP notions used by the delineator are not fully accepted by reviewers and stakeholders.

An example of the TCP mapping is illustrated for the area just downstream of Long Bar (~ RKM 22.5 – 24.0) in Figure 6. This example was created with the workflow in Figure 4 using ArcGIS v. 10 (ESRI, Redlands, CA) to segment the rasters based on the decision tree criteria in Figure 5; however, other preferred programming methods for automating the delineation are widely available and may be employed at the user's discretion.

Spatial abundance and distribution

To characterize the abundance and distribution of TCPs, aggregate areal statistics were computed and the longitudinal profile of abundance analyzed. To calculate the abundance of each TCP type in the LYR, the planform area of each individual TCP polygon was calculated in ArcGIS. Polygon areas were summed by type and divided by the total study area to determine percent coverage. Longitudinal distributions were calculated as the percent area of each TCP type within cross sectional rectangles distributed down the river. To define cross sections, the river valley centerline was automatically stationed in ArcGIS and given perpendicular cross sections evenly every 6 m (~ 1/10 base-flow width) along the study segment. Cross sections were then buffered 3 m upstream and downstream to create rectangles that spanned the wetted width and contiguously covered the segment area. Within each rectangle, the areas of each TCP type were calculated and converted to a percent of total TCP type area, and those areas were assigned to the cross section at each rectangle's center. Longitudinal distributions are presented as discrete area functions.

Rate of depth changes

At the segment scale, the mean net vertical change was computed for each TCP. The DoD raster provides the change in topographic height (scour, fill, or no change) for each pixel between 1999 and 2006/2008. Therefore, mean net vertical changes were calculated as the averages of each pixel value among all polygons for each TCP type.

For the special case of the LYR, whose DoD raster was created from two different time epochs between surveys (seven years for TBR, and nine years for the rest of the segment), converting the mean TCP depths to annual rates was not as simple as dividing by a single time span because the values could not be summed across that epoch difference. Instead, the rates of depth changes were calculated after the rates of volume changes were calculated (described in more detail in the following sub-section). Because the total volume changes can be summed across the two survey epochs, the mean annual depth changes were calculated as the quotients of the mean annual volume changes and the areas for each TCP type.

Annual sediment budget by TCP

For each TCP type the sum of topographic change heights was computed and multiplied by the planform area of that TCP. Wheaton et al. (2013) chose to apply the same kind of volumetric calculation (i.e. cell-by-cell LoD summation times TCP area) to the level of detection (LoD) raster from spatially explicit uncertainty analysis to obtain an estimate of volumetric uncertainty. However, they noted that this is an overly aggressive calculation that excludes from consideration a significant amount of real topographic change. It remains to be determined what are technically sound and scientifically meaningful approaches for spatially explicit volumetric uncertainty analysis in different settings, so no such procedure was used herein.

In order to convert the absolute volumetric change to an annual budget, the calculation had to be performed in two steps because the time epoch for Timbuctoo Bend is different than the rest of the river. First, the TCP map was split into the two regions: within Timbuctoo Bend (i.e. the 2006 dataset), and everything else. The Timbuctoo Bend TCP map was used to calculate the mean vertical change for each process type, and the same was done for the TCP map of the rest of the alluvial river. The total areas of each process type within each map were also determined in ArcGIS. The mean depths for each region were divided by the time epoch (seven years for Timbuctoo Bend, and nine years for the rest). These mean annual depth changes were multiplied by the total area of each TCP within each region and then summed between the two regions.

Results

Spatial abundance and distribution

The full 34-km TCP map is provided as a supplemental material to allow for inspection of the pattern along the whole river segment (Supplemental Figure 2). At the segment scale, nearly half of the area (46.9%) experienced no detectable net elevation change over the survey epochs. The remaining 53.1% of the area that did experience measurable change were classified into one of 19 TCP types (Figure 7). The LYR exhibited a highly unequal abundance of types, with five (overbank storage, overbank scour, vegetated overbank storage, downcutting, and in-channel fill) comprising of about 76% of the areas that experienced change (but only ~40% of the total segment area). The five least abundant processes (island removal, abandoned channel infill, cohesive bank retreat, island scour, and island emergence) combined comprised <0.75% of the total area, suggesting that those processes were highly localized.

The longitudinal organization of each TCP type showed that most of the processes were located non-randomly within the LYR (Figure 8, for most pertinent TCP types; Supplemental Figure 3, for all TCP types). Even the most abundant process, overbank storage, was dominant in the regions just downstream of DPD and was mostly lacking in the regions just upstream of DPD (Figure 8A), which was already full of sediment and thus not the typical control on TCPs presented by dams. The most ubiquitously organized processes were non-cohesive bank migration (Figure 8E) and downcutting (Figure 8C). Many of the lesser abundant processes only occurred in a few locations along the valley (e.g. cohesive bank retreat, Figure 8F).

Within the 1999 wetted channel, the most abundant processes were downcutting (Figure 8C), bar emergence (Figure 8G), and in-channel fill (Figure 8D). The high abundance of bar emergence processes in the LYR suggests that the river allows for meander and re-mobilisation of floodplain sediments. Bars emerge as channels migrate and consume old floodplain, which keeps new floodplain geometry in a state of self-maintenance with the flow regime (see Discussion section for more details). The most abundant processes outside of the 1999 wetted channel were overbank storage (Figure 8A), overbank scour (Figure 8B), and vegetated overbank storage (Figure 8H).

Rate of depth changes

The mean depths of changes within each TCP can be more relevant for those processes that cover small total areas, but produce locally large volume differences (Figure 9). Overbank scour processes exported the majority of the LYR sediment; however, those processes were widespread. The mean annual depth change for overbank scour was –10.26 cm/yr. Cohesive bank retreat, on the other hand, occurred in only a few small locations along the channel and scoured less than 1% of the total volume; however, the mean annual depth changes in those regions were –32.08 cm/yr, almost three times those of overbank scour. Therefore, while cohesive bank retreat processes were not very important at the segment scale, they were highly relevant at the scale of 0.1-10 channel widths. Among the fill processes, overbank storage comprised the most area and volume at the segment scale, but the mean annual depth changes within those regions were a rather pedestrian +7.37 cm/yr as compared to abandoned channel infill processes that exhibited a mean depth change of more than triple that (+25.65 cm/yr). Locally, the most dynamic processes were cohesive bank retreat, berm scour & mass failure, avulsion, noncohesive bank migration, abandoned channel infill, bar emergence, and island removal.

Annual sediment budget

The three most abundant TCPs (overbank storage, overbank scour, and vegetated overbank storage) also created the most volume of topographic changes within the segment scale (Figure 10). Considering the absolute volume of sediment displaced (eroded or deposited) by all processes, overbank storage was the most dominant (~15.4%), followed by overbank scour (~15.1%) and vegetated overbank storage (~14.9%). Island scour and island removal processes were among the least abundant types, and they also were responsible for the least volumes of sediment displacement as well.

Discussion

Methodological developments

The hierarchical segmentation method used herein is based on a decision tree analysis that has previously been shown to outperform other classification algorithms, such as linear discriminant and maximum likelihood functions, in classifying remotely sensed land cover data (Friedl and Brodley, 1997), satellite imagery of vegetation (Laliberte *et al*., 2007), susceptibility to landslides (Saito *et al*., 2009), and channel landforms (Wyrick *et al*., 2014). The TCP decision tree was created with internal expert decisions that then automatically and objectively created a polygon map of segmented TCP types. Even though this method includes subjectivity in designing the tree, those decisions are fully transparent and easily adjustable for any DoD dataset. Thus, the method yields an objective map of TCP polygons free of field observer bias and is open to future revision, unlike decisions made in the field. The automation also allows for analysis of systems at multiple scales, up to and including the catchment scale that previously would have been onerous with hand-mapping methods.

Another benefit of this automated procedure is that it allows for a more diverse, complex, and accurate view of the topographic changes within a river valley to emerge. On the LYR, almost half of the area did not experience detectable topographic change. Within the areas that did change, five TCPs dominated, occurring over three-fourths of that area (Figure 7). Thus, allowing for up to 19 processes did not preclude a small subset from revealing themselves as most widespread, and it enabled the revelation of important locations of unique changes that promote fluvial diversity. The five abundant processes did not occur uniformly across the segment. Some, like overbank storage and in-channel fill, were more abundant in the lower half, while others, like overbank scour and downcutting, were more abundant in the upper half of the segment (Figure 8). Additionally, none of these five most abundant TCPs ranked in the top half of mean depths (Figure 9). This begins to paint a picture that the relative impact of various TCPs relies heavily on the scale of the study. A certain process, such as cohesive bank retreat, can be a relatively minor player at the segment scale, but a dominant player at the 1- 10 channel widths scale (Figure 10). The decision tree methodology presented herein enables this detailed view because it removes any pre-suppositions of the observer and can be applied to any scale.

LYR geomorphologic conceptualization

The results presented herein represent an analysis of the topographic changes that occurred between 1999 and 2006/2008 along the LYR valley, which is the period from 58-67 years after the valley was cut off from its historic sediment supply. It is, therefore, not recommended that these results be used to infer specific temporal changes within the valley corridor outside of that time epoch relative to the post-dam era. Prior historical changes to the LYR valley were previously reported (James *et al.*, 2009), but could not be assessed at the resolution used in this study. However, it is possible to make some generalizations about the LYR channel based on these results, namely in the context of morphologic self-maintenance.

By the 1880's hydraulic mining had deposited an estimated 253 million m^3 of sediment in the low-gradient LYR valley below the modern Englebright Dam (Gilbert, 1917). The depth of aggradation was estimated to be about 17 m above bedrock (Gilbert, 1917; James *et al*., 2009). The LYR channel at this time was prone to avulsions, braiding, and anabranching (James *et al*., 2009). As part of a management plan in 1906 to minimize the sediment influx downstream of the LYR, the levee spacings were widened to ~ 4 km that then narrowed to ~ 600 m near the mouth, which resulted in a stabilized channel location (James *et al*., 2009). The Englebright Dam was installed in 1941. Based on analysis of thalweg elevation profiles in historic and 1999 maps, James *et al*. (2009) determined that the thalweg experienced vertical incision throughout its length, except for the reach immediately upstream of DPD which experienced mostly lateral migration. This result might fit well into the expectations of an incising river downstream of a dam; however, it is an incomplete story of the geomorphic changes because it does not consider the channel as a whole, let alone what is happening on the floodplains. Thalwegs have commonly been used as a surrogate in the absence of DEMs, but now it is possible to see the full lateral spatial dynamic. From 1999 to 2006/2008, the out-of-channel regions also experienced scour at similar rates as the in-channel regions (e.g. Figure 6; supplemental figure). Downstream of DPD, which experienced most of the deposition (supplemental figure) as predicated by the large levee spacing, the main channel meandered through the sediments, filling in its old channel and laterally scouring through the floodplain (e.g. Figure 8).

Unexpected channel fill downstream of dam

According to long-standing conventional theory and observation, the river segment downstream of a dam should be downcutting with an increasing disconnection between channel and floodplain through time (Petts, 1979; Williams, 1978). Most studies have looked for only a brief period after dams are installed, so how this plays out decades to centuries later remains unclear. Large dams retard the downstream movement of sediments, typically causing the downstream flow to have greater transport capacity than carrying load, thus the downstream channel bed incises (e.g. Brandt, 2000). This degradation is generally more pronounced when dams have little effect on the flood peaks (Williams and Wolman, 1984). Dams also tend to decrease meander rates (e.g. Friedman *et al*., 1998; Shields Jr., *et al*., 2000), allowing for more channel incision and less floodplain interaction. Low-resolution, historic DoD analyses on the LYR showed some initial incision within the main channel and high-water channels after the Englebright Dam was installed (James *et al*., 2010).

The results of this study present a different outcome ~ 67 years after dam installation that challenges the dogmatic application of the standard concept regardless of local context and time. Specifically, even though the whole regulated downstream river valley was net erosional and thus not graded during the study epoch, the 1999 channel was dominated by fill processes in the subsequent 7-9 years, whereas scour processes dominated overbank. Specifically, there was 165,100 m^3 of net fill in the channel and 191,600 m^3 of net scour overbank (Table 2). Outside of the 1999 channel, overbank scour processes were the dominant TCP type, with some noncohesive bank migration processes as well, which hints at a diversity of lateral and vertical processes at work in the LYR. Additionally, vertical scour rates are similar for overbank and in-channel regions, because these regions are served by different processes of similar capability. These results show that even in an erosion-dominated regulated valley, the channel need not become disconnected from the floodplain, but instead can exhibit TCPs more like a well-connected system (Wolman and Leopold, 1957).

There are several reasons why the river has not experienced a singular in-channel incision as commonly expected. First, the flow regime is still fairly dynamic for a regulated river, with overbank flows occurring every ~ 1.25 years (Wyrick and Pasternack, 2012), and flow heterogeneity is known to promote process diversity (Parker *et al*., 2003). Second, the absence of cohesive mud in much of the surficial bed material and the associated presence of large tree root wads limit the height of banks before lateral mass wasting occurs, thereby promoting widening over incision and disconnection. Third, the bed surface becomes armored when there are more than ~ 4 years between large floods, as there are diverse in-channel flows and small overbank floods that are capable of partial transport most years. The armored bed consists of coarse gravel and cobble, while steep banks are composed of a heterogenous mixture with abundant fine gravel and sand. Combined with flow asymmetry impinging on and undercutting steep banks, this promotes bank erosion before bed erosion for any given discharge (Parker, 1979; Knighton, 1998). Finally, this study did not solely look at change along the thalweg, as commonly done in the classic studies, but instead assessed the planform spatial complexity of TCPs. From this viewpoint, it may be that all regulated rivers are more dynamic than thought, just the viewpoint was too narrow, or it may be that the LYR is a unique outlier, especially given the unique presence of a large amount of valley fill due to influx of hydraulic mining sediment prior to damming.

The dynamism of the LYR thus brings up the question of whether the valley is still adjusting to Englebright Dam, or has it already adjusted and is now just shifting around. The conclusion of Carley *et al*. (2012) was that the channel is still adjusting upstream of DPD, which is verified by the results of James *et al*. (2009) showing that that section has not yet downcut. Downstream of DPD, the LYR is trying to digest and transport the sediment volumes scoured from upstream.

Scouring floodplains

In terms of overbank scour, this study found that when the appropriate factors are in play, a regulated river can systematically evacuate its excessive storage of sediment at the valley scale without disconnecting channel and floodplain. In this case, four key factors appear to be at work: two externally and two internally determined. The two external factors that are already well understood in the literature are (1) requisite discharge to overflow onto the floodplain with enough force to cause topographic change and (2) a lower base level to strive toward. The two internal factors relate to the role of vegetation and are not as well understood, hence more discussion is offered for those.

Drawing on the LiDAR-derived vegetation data from Abu-Aly *et al*. (2013), 25% of the LYR corridor is vegetated within the 1195 m^3/s wetted area (~ 8 times bankfull flow) of which half occurs along the channel margin and half overbank. The relative abundance of vegetation along the banks is linked to proximal access to shallow groundwater and is common for semi-arid cobble-gravel streams. This vegetation usually hinders geomorphic dynamism in regulated rivers, especially where sand supply is high and flow regulation severe (Marston *et al*., 1995; Polzin and Rood, 2000; USDI, 2000; Edwards, 2004). However, on the Yuba, sand and mud supply are low and flow regulation during floods modest. As a result, lateral TCPs were observed to effectively overcome vegetation by migration and avulsion. Processes like cohesive bank retreat and noncohesive bank migration were found capable of mining under the roots of willows and cottonwoods. Although too ephemeral to be classified in this study, knickpoint migration has been observed on the LYR on the event scale and can also undermine vegetation on medial bars. In contrast, sub-avulsion and avulsion directly attack vegetation from the top and rip it out completely as part of the process of finding a more direct route downslope when that route is more orthogonal to the primary axis of streambank vegetation, such as at river bends. Where flow is parallel to riverbank vegetation, only the canopies are ripped out; the roots and stems remaining intact and actually accrete coarse sediment (Sawyer *et al*., 2010). For example, in the New Years 2006 flood with a peak of 3126 m^3/s, thick riparian patches were cut through by avulsions at focused locations, while neighboring patches experienced substantial deposition. Thus, the occurrence of modest vegetation coverage plays a significant role in enabling floods to continue to evacuate hydraulic-mining deposits from the river valley over decades, while also promoting hydraulic and geomorphic complexity for ecological functions.

Conclusions

The primary goal of this project was to comprehensively and transparently delineate and map the topographic changes that occurred in the LYR over a 7-9 year epoch, as well as characterize the specific processes that created those changes. A combination of dense datasets, novel data-processing methods, and GIS-based spatial analyses were utilized to achieve this goal. Topographic change processes are rarely analyzed at the segment-scale; instead, studies have generally focused on the site-scale. This study, however, used a near-census (~ 1-m resolution) approach for differencing two DEM datasets and identifying regions of change and the specific mechanisms that caused those changes. The use of near-census datasets in analyses have been shown to produce more detailed characterizations of river corridor processes and to be more accurate across multiple scales (Pasternack, 2011). Difference of DEMs results were used to analyze the spatial patterns of topographic changes within the LYR valley, as well as infer indicators of channel self-maintenance. New methods were developed to identify and delineate specific processes of topographic change at multiple scales.

This study highlights several key advances to the science and analysis of identifying topographic change processes. First, using two sets of available DEMs, the 37-km valley segment was categorized into regions of scour, fill, and no detectable change based on the differences in topographic elevations between the two surveys. Conventional wisdom would hypothesize that topographic changes downstream of a sediment-barrier dam would be dominated by in-channel vertical scour, thus entrenching the flow and exacerbating the disconnect between the channel and its floodplains. However, the opposite occurred in the LYR ~ 65 years after damming – even though the river valley was net erosional, the 1999 channel area experienced net fill, while the out-of-channel regions experienced net scour over the survey epochs. Second, starting from a 1.5-m resolution DoD raster, it was possible to identify a suite of 19 distinct processes of topographic change that serve as the fundamental creators of the current morphology. The ability to quickly and transparently map TCPs for a segment of this scale represents a scientific advancement that is primarily due to the availability of the near-census input datasets. The exact terminology of the TCP types may differ from those used in past or future studies, but that is not important. What is scientifically novel is the new methodology implemented to map the processes and the ability to interpret them over multiple spatial scales.

The changes reported herein represent only those that occurred between 1999 and 2006/2008. Therefore, these data should be used as a baseline to describe what happened to create the conditions necessary for any post-2008 datasets by which to stratify. The characterizations of topographic changes can be used as a comparable context for historic or future DoD studies.

Acknowledgments

Primary funding for this study was provided by the Yuba County Water Agency (Award #201016094), the Yuba Accord River Management Team, and the USDA National Institute of Food and Agriculture (Hatch project number #CA-D-LAW-7034-H). We thank anonymous reviewers for input that improved the manuscript.

References

Abu-Aly TR, Pasternack GB, Wyrick JR, Barker R, Massa D, Johnson T. 2013. Effects of LiDAR-derided, spatially-distributed vegetative roughness on 2D hydraulics in a gravel-cobble river at flows of 0.2 to 20 times bankfull. *Geomorphology*. DOI:10.1016/j.geomorph.2013.10.017.

Allen JRL. 1965. A review of the origin and character of recent alluvial sediments. *Sedimentology* **5**: 89-91.

Barker JR. 2010. Lower Yuba River QA/QC comparison: LIDAR data, boat echo sounder data, NGS benchmarks, total station and RTK-GPS survey points. Prepared for the Yuba Accord River Management Team, Marysville, CA.

Barker JR. 2011. Rapid, abundant velocity observations to validate million-element 2D hydrodynamic models. MS Thesis, University of California, Davis, Davis, CA.

Barker R, Dixon L, Hooke J. 1997. Use of terrestrial photogrammetry for monitoring and measuring bank erosion. *Earth Surface Processes and Landforms* **22 (13)**: 1217-1227.

Bishop MP, James LA, Shroder Jr. JF, Walsh SJ. 2012. Geospatial technologies and digital geomorphological mapping: concepts, issues and research. *Geomorphology* **137**: 5-26.

Brandt SA. 2000. Classification of geomorphological effects downstream of dams. *Catena* **40**: 375-401.

Brasington J, Rumsby BT, McVey RA. 2000. Monitoring and modelling morphological change in a braided gravel-bed river using high resolution GPS-based survey. *Earth Surface Processes and Landforms* **25 (9):** 973-990.

Carley JK, Pasternack GB, Wyrick JR, Barker JR, Bratovich PM, Massa DA, Reedy GD, Johnson TR. 2012. Significant decadal channel change 58-67 years post-dam accounting for uncertainty in topographic change detection between contour maps and point cloud models. *Geomorphology* **179**: 71-88.

Costa BM, Battista TA, Pittman SJ. 2009. Comparative Evaluation of Airborne LiDAR and Ship-Based Multibeam SoNAR Bathymetry and Intensity for Mapping Coral Reef Ecosystems. *Remote Sensing of Environment* **113**: 1082–1100.

Curtis JA, Flint LE, Alpers CN, Yarnell SM. 2005. Conceptual model of sediment processes in the upper Yuba River watershed, Sierra Nevada, CA. *Geomorphology* **68**: 149–166.

Darby SE, Rinaldi M, Dapporto S. 2007. Coupled simulations of fluvial erosion and mass wasting for cohesive river banks. *Journal of Geophysical Research* **112**: F03022, DOI:10.1029/2006JF000722.

Das T, Dettinger M, Cayan D, Hidalgo H, 2011, Potential increase in floods in California's Sierra Nevada under future climate projections. *Climatic Change* **109 (Suppl 1):** 71-94.

Edwards BR. 2004. Historical assessment of the ecological condition and channel dynamics of the lower Mokelumne River: 1910-2001. MS Thesis, Humboldt State University, Arcata, CA.

Ferguson RI, Ashmore PE, Ashworth PJ, Paola C, Prestegaard KL. 1992. Measurements in a braided river chute and lobe: 1. Flow pattern, sediment transport, and channel change. *Water Resources Research* **28 (7)**: 1877-1886.

Friedl MA, Brodley CE. 1997. Decision tree classification of land cover from remotely sensed data. *Remote Sensing of Environment* **61**: 399-409.

Friedman JM, Osterkamp WR, Scott ML, Auble GT. 1998. Downstream effects of dams on channel geometry and bottomland vegetation: regional patterns in the Great Plains. *Wetlands* **18 (4)**: 619-633.

Fuller IC, Large ARG, Charlton ME, Heritage GL, Milan DJ. 2003. Reach-scale sediment transfers: an evaluation of two morphological budgeting approaches. *Earth Surface Processes and Landforms* **28**: 889-903.

Fuller IC, Basher LR. 2013. Riverbed digital elevation models as a tool for holistic river management: Motueka River, Nelson, New Zealand. *River Research and Applications* **29 (5)**: 619-633.

Gilbert GK. 1917. Hydraulic-mining debris in the Sierra Nevada. US Geological Survey Professional Paper 105, Washington DC.

Goff JR, Ashmore P. 1993. Gravel transport and morphological change in braided Sunwapta River, Alberta, Canada. *Earth Surface Processes and Landforms* **19 (3)**: 195-212.

Grabowski RC, Surian N, Gurnell AM. 2014. Characterizing geomorphological change to support sustainable river restoration and management. *WIREs Water* **1**: 483-512.

Gurnell AM, Petts GE. 2002. Island-dominated landscapes of large floodplain rivers, a European perspective. *Freshwater Biology* **47**: 581-600.

Hadley RF, Schumm SA. 1961. Sediment sources and drainage basin characteristics in Upper Cheyenne River Basin. USGS Water-Supply Paper 1531-B.

Hall RK, Watkins RL, Heggem DT, Jones KB, Kaufmann PR, Moore SB, Gregory SJ. 2009. Quantifying structural physical habitat attributes using LIDAR and hyperspectral imagery. *Environmental Monitoring and Assessment* **159**: 63-83.

Heritage GL, Milan DJ, Large RG, Fuller IC. 2009. Influence of survey strategy and interpolation model on DEM quality. *Geomorphology* **112**: 334-344.

Hilldale RC, Raff D. 2008. Assessing the ability of airborne LiDAR to map river bathymetry. *Earth Surfaces Processes and Landforms* **33**: 773–783. DOI: 10.1002/esp.1575.

Horne GS, Patton PC. 1989. Bedload-sediment transport through the Connecticut River estuary. *Geological Society of America Bulletin* **101 (6)**: 805-819.

Jackson J, Pasternack GB, Wyrick JR. 2013. Substrate of the lower Yuba River. Prepared for the Yuba Accord River Management Team. University of California, Davis, 53 pp.

James LA, Singer MB, Ghoshal S, Megison M. 2009. Historical channel changes in the lower Yuba and Feather Rivers, California: long-term effects of contrasting river-management strategies. In *Management and Restoration of Fluvial Systems with Broad Historical Changes and Human Impacts*, James LA, Rathburn SL, Whittecar GR (eds). Geological Society of America Special Paper 451: 57–81. DOI:10.1130/2008.2451(04).

James LA, Hodgson ME, Ghoshal S, Latiolais MM. 2010. Geomorphic change detection using historic maps and DEM differencing: the temporal dimension of geospatial analysis. *Geomorphology* **137 (1)**: 181-198.

Javernick L, Brasington J, Caruso B. 2014. Modeling the topography of shallow braided rivers using Structure-from-Motion photogrammetry. *Geomorphology* **213**: 166-182.

Knighton D. 1998. Fluvial Forms and Process: A New Perspective. Arnold: London.

Laliberte AS, Fredrickson EL, Rango A. 2007. Combining decision trees with hierchical object-oriented image analysis for mapping arid rangelands. *Photogrammetric Engineering and Remote Sensing* **73 (2)**: 197-207.

Lane SN, Richards KS, Chandler JH. 1994. Developments in monitoring and modeling small-scale river bed topography. *Earth Surface Processes and Landforms* **19 (4)**: 349-368.

Leopold LB, Wolman MG, Mille, JP. 1964. Fluvial Processes in Geomorphology. W.H. Freeman: San Francisco, CA, USA.

Marston RA, Girel J, Pautou G, Piegay H, Bravard J, Arneson C. 1995. Channel metamorphosis, floodplain disturbance, and vegetation development: Ain River, France. *Geomorphology* **13**: 121-131.

Merz JE, Pasternack GB, Wheaton JM. 2006. Sediment budget for salmonid spawning habitat rehabilitation in the Mokelumne River. *Geomorphology* **76 (1-2)**: 207-228.

Moir HJ, Pasternack GB. 2010. Substrate requirements of spawning Chinook salmon (*Oncorhynchus tshawytscha*) are dependent on local channel hydraulics. *River Research and Applications* **26**: 456-468.

Moore ID, Grayson RB, Ladson AR. 1991. Digital terrain modelling: a review of hydrological, geomorphological and biological applications. *Hydrological Processes* **5**: 3-30.

Nanson GC. 1986. Episodes of vertical accretion and catastrophic stripping: a model of disequilibrium flood-plain development. *Geological Society of America* **97 (12)**: 1467-1475.

Nicholas AP. 2013. Modelling the continuum of river channel patterns. *Earth Surface Processes and Landforms* **38**: 1187–1196. DOI:10.1002/esp.3431.

Parker G. 1979. Hydraulic geometry of active gravel rivers. *Journal of the Hydraulics Division American Society of Civil Engineers* **105 (HY9)**: 1185-1201.

Parker G, Toro-Escobar CM, Ramey M, Beck S. 2003. The effect of floodwater extraction on the morphology of mountain streams. *Journal of Hydraulic Engineering* **129 (11)**: 885-895.

Pasternack GB. 2008. SHIRA-based river analysis and field-based manipulative sediment transport experiments to balance habitat and geomorphic goals on the Lower Yuba River. Cooperative Ecosystems Studies Unit (CESU) 81332 6 J002 Final Report: University of California at Davis, Davis, CA.

Pasternack GB. 2011. 2D Modeling and Ecohydraulic Analysis. Createspace: Seattle, WA, USA.

Pasternack GB, Tu D, Wyrick JR. 2014. Chinook adult spawning physical habitat of the lower Yuba River. Prepared for the Yuba Accord River Management Team. University of California, Davis, 154 pp.

Petts GE. 1979. Complex response of river channel morphology to reservoir construction. *Progress in Physical Geography* **3**: 329-362.

Polzin ML, Rood SB. 2000. Effects of damming and flow stabilization on riparian processes and black cottonwoods along the Kootenay River. *Rivers* **7**: 221-232.

Rosgen D. 1996. Applied River Morphology. Wildland Hydrology: Pagosa Springs, CO, USA.

Rubin DM, Schmidt JC, Moore JN. 1990. Origin, structure, and evolution of a reattachment bar, Colorado River, Grand Canyon, Arizona. *Journal of Sedimentary Petrology* **60 (6)**: 982-991.

Saito H, Nakayama D, Matsuyama H. 2009. Comparison of landslide susceptibility based on a decision-tree model and actual landslide occurrence: The Akaishi Mountains, Japan. *Geomorphology* **109 (3-4)**: 108-121.

Sawyer AM, Pasternack GB, Merz JE, Escobar M, Senter AE. 2009. Construction constraints on geomorphic-unit rehabilitation on regulated gravel-bed rivers. *River Research and Applications* **25**: 416-437.

Sawyer AM, Pasternack GB, Moir HJ, Fulton AA. 2010. Riffle-pool maintenance and flow convergence routing confirmed on a large gravel bed river. *Geomorphology* **114**: 143-160.

Shields Jr FD, Simon A, Steffen LJ. 2000. Reservoir effects on downstream river channel migration. *Environmental Conservation* **27 (1)**: 54-66.

Singer MB, Aalto, R, James LA, Kilham NE, Higson JL, Ghoshal S. 2013. Enduring legacy of a toxic fan via episodic redistribution of California gold mining debris. *Proceedings of the National Academy of Sciences* **110 (46)**: 18436-18441.

Slingerland R, Smith ND. 1998. Necessary conditions for a meandering-river avulsion. *Geology* **26 (5)**: 435-438.

Storer TI, Usinger RL, Lukas D. 2004. Sierra Nevada Natural History (revised ed.). University of California Press: Berkeley, CA, USA.

U.S. Department of Interior. 2000. Record of decision, Trinity River mainstem fishery restoration final environmental impact statement/environmental impact report. Decision by the U.S. Department of Interior, December 2000.

Warburton J, Davies TRH, Mandl MG. 1993. A meso-scale field investigation of channel change and floodplain characteristics in an upland braided gravel-bed river, New Zealand. *Geological Society of London, Special Publications* **75 (1)**: 241-255.

Wheaton JM, Brasington J, Darby SE, Sear D. 2010a. Accounting for uncertainty in DEMs from repeat topographic surveys: improved sediment budgets. *Earth Surface Processes and Landforms* **35 (2)**: 136-156.

Wheaton JM, Brasington J, Darby S, Merz JE, Pasternack GB, Sear DA, Vericat D. 2010b. Linking geomorphic changes to salmonid habitat at a scale relevant to fish. *River Research and Applications* **26**: 469-486.

Wheaton JM, Brasington J, Darby SE, Kasprak A, Sear D, Vericat D. 2013. Morphodynamic signatures of braiding mechanisms as expressed through change in sediment storage in a gravel-bed river. *Journal of Geophysical Research: Earth Surface* **118 (2)**: 759-779.

White JQ, Pasternack GB, Moir HJ. 2010. Valley width variation influences riffle-pool location and persistence on a rapidly incising gravel-bed river. *Geomorphology* **121**: 206-221.

Williams GP, Wolman MG. 1984. Downstream effects of dams on alluvial rivers. U.S. Geological Survey Professional Paper 1286.

Williams GP. 1978. The case of the shrinking channels – the North Platte and Platte Rivers in Nebraska. United States Geological Survey Circular 781.

Wilson JP. 2012. Digital terrain modeling. *Geomorphology* **137**: 107-121.

Wolman MG, Leopold LB. 1957. River Flood Plains: Some Observations on their Formation. United States Geological Survey Professional Paper 282-C.

Wyrick JR, Klingeman PC. 2011. Proposed fluvial island classification scheme and its use for river restoration. *River Research and Applications* **27**: 814-825.

Wyrick JR. Pasternack GB. 2012. Landforms of the Lower Yuba River. Prepared for the Yuba Accord River Management Team. University of California, Davis, CA.

Wyrick JR, Senter AE, Pasternack GB. 2014. Revealing the natural complexity of fluvial morphology through 2D hydrodynamic delineation of river landforms. *Geomorphology* **210**: 14-22.

Wyrick JR, Pasternack GB. 2014. Geospatial organization of fluvial landforms in a gravel-cobble river: beyond the riffle-pool couplet. *Geomorphology* **213**: 48-65.

Yumoto M, Ogata T, Matsuoka N, Matsumoto E. 2006. Riverbank freeze-thaw erosion along a small mountain stream, Nikko volcanic area, central Japan. *Permafrost and Periglacial Processes* **17 (4)**: 325-339.

944 **Table 1a**. Qualitative descriptions of fill topographic change processes mapped in the

945 LYR

Process	Definition
Abandoned channel in-fill	There are two mechanisms that could create this region, but they are indistinguishable without more knowledge of the river within the time epoch. First, the region could have experienced enough deposition that the channel was re-routed through another location within the floodplains. Or the wetted channel changed location due to other processes (e.g. avulsion), and these regions subsequently experienced deposition from overbank floods. In either case, these regions are no longer adjacent with the wetted channel.
Bar emergence	Unvegetated region that are formed by enough deposition in recirculation zones at channel expansions to become exposed and subsequently push the wetted channel towards the opposite bank. These regions are still adjacent to current wetted channel, and become incorporated into the floodplain as the channel migrates. The resultant structure is generally identified as a type of bar (e.g. lateral or point) and exhibit slopes towards the channel.
Berm Fill	Regions along the training berms that experienced deposition. These are distinguished from overbank storage processes because training berms and other mining deposits are generally taller than the flows (i.e. never completely submerged).
In channel fill	Region within the wetted channel that experienced deposition due to flow recirculation or channel widening, but not enough to become emergent or change the location of the wetted channel.
Island emergence	Region within the wetted channel that experienced enough deposition to become emergent. The new flow paths now separate around this deposition and isolate it from the floodplains.
Island storage	Unvegetated region that has been continuously emergent and isolated from the floodplains within the time epoch, and has experienced deposition from overbank floods.
Overbank storage	Unvegetated region outside of the wetted channel that act as a sediment sink due to flow expansion and decreased velocities. No particular pattern is noticeable.
Vegetated bar emergence	Same as the bar emergence process, but occurs within a vegetated area.
Vegetated island storage	Same as the island storage process, but occurs within a

	vegetated area.
Vegetated overbank storage	Same as the overbank storage process, but occurs within a vegetated area.

Table 1b. Qualitative descriptions of scour topographic change processes mapped in the LYR

Process	Definition
Avulsion	Complete shift, usually abrupt, in channel position through the floodplains that is separated from the previous wetted channel. Generally triggered as overbank flows scour a topographic low or crevasse in floodplain to a lower elevation than the original channel.
Cohesive bank retreat	Progressive lateral movement of the channel through cohesive bank material (i.e. with high clay content or vegetation) by means of weathering/weakening, fluvial entrainment, and/or mass wasting. The cohesiveness of the material leads to near-vertical banks and abrupt transitions between the channel and floodplain.
Downcutting	Region that experienced vertical erosion within the wetted channel. These regions are continually wetted within the time epoch.
Island removal	Region that was previously emergent and isolated from the floodplains, but experienced enough erosion due to overbank floods to now become submerged within the wetted channel.
Island scour	Region that has been continuously emergent and isolated from the floodplains, and experienced erosion from overbank floods, but not enough to become submerged.
Noncohesive bank migration	Progressive lateral movement of the channel through non-cohesive material of the floodplains by means of weathering/weakening, fluvial entrainment, and/or mass wasting. The non-cohesiveness leads to slumping of the banks, thus maintaining a gradually-sloped transition from channel to floodplain.
Overbank scour	Region outside of the wetted channels that experienced erosion during overbank floods due to macro- or micro-scale hydraulic controls. No particular pattern is noticeable.
Berm scour & mass wasting	Region along the training berms that experience scour. This is distinguished from the Noncohesive Bank Migration because training berms and other mining deposits are generally taller than the flows (i.e. never completely submerged). However, flows can erode the lower portions

	of the berms and thus create slumping of the berm tops (which are identified as erosion in the DoD) due to the noncohesiveness of the material.
Sub-avulsion	Streamwise longitudinal scour in the floodplain regions, usually parallel to the wetted channel, that is formed during overbank flows, but has not connected a separate low-flow pathway (like avulsion). These regions are usually attached to the wetted channel at either the exit or entrance, but not both and not continuously adjacent along its length. It is presumed that future overbank floods will continue this erosive pattern and eventually create an avulsion in that location.

Table 2. Absolute volumetric changes of the in-channel and out-of-channel topography

	Out-of-channel		In-channel	
	TCP	Volume (m^3)	TCP	Volume (m^3)
Fill Processes	Overbank storage	772,500	In-channel fill	381,800
	Vegetated overbank storage	751,500	Bar emergence	135,000
	Berm fill	127,700	Vegetated bar emergence	51,100
	All others	179,400	All others	46,500
Scour Processes	Overbank scour	-732,700	Downcutting	-449,200
	Non-cohesive bank migration	-610,700	Island removal	-16,500
	Berm scour & Mass failure	-438,000		
	All others	-241,300	All others	0

Figure Captions

Figure 1. Yuba River watershed setting and lower Yuba River landmarks

Figure 2. Hydrograph of mean daily discharge at Marysville showing flows during the times of surveys

Figure 3. Workflow for creating DoD raster in ArcGIS 10.0 based on methodology from Carley *et al*. (2012)

Figure 4. Workflow for applying the decision tree approach to TCP delineation and identification. This method assumes the use of ArcGIS v. 10; however, other preferred programming methods for automating the delineation may be employed at the user's discretion.

Figure 5. Decision tree for delineating topographic change processes within the LYR valley. Delineation begins on the left of this figure with the Fill or Scour raster. Definitions of each TCP type are provided in Table 1.

Figure 6. Example of TCP delineation within the LYR. (A) satellite imagery from 2009. (B) regions of in-channel and out-of-channel based on 1999 and 2006/2008 wetted areas. (C) regions of scour, fill, and no detectable change. (D) TCP map.

Figure 7. Segment-scale abundance percentages of TCP types in the LYR

Figure 8. Longitudinal patterns of discrete area fractions for eight of the TCP types in the LYR. Refer to Supplemental Figure 3 for the longitudinal patterns of all types.

Figure 9. Mean annual changes in topographic depths for TCP types in the LYR

Figure 10. Annual rates of volumetric changes per TCP type in the LYR

Supplemental Figure 1. Segment-scale map of DEM differences on the LYR between 1999 and 2006 (Timbuctoo Bend only) and 2008 (all other regions)

Supplemental Figure 2. Segment-scale map of topographic change processes on the LYR

Supplemental Figure 3. Longitudinal patterns of discrete area fractions for all TCP types in the LYR

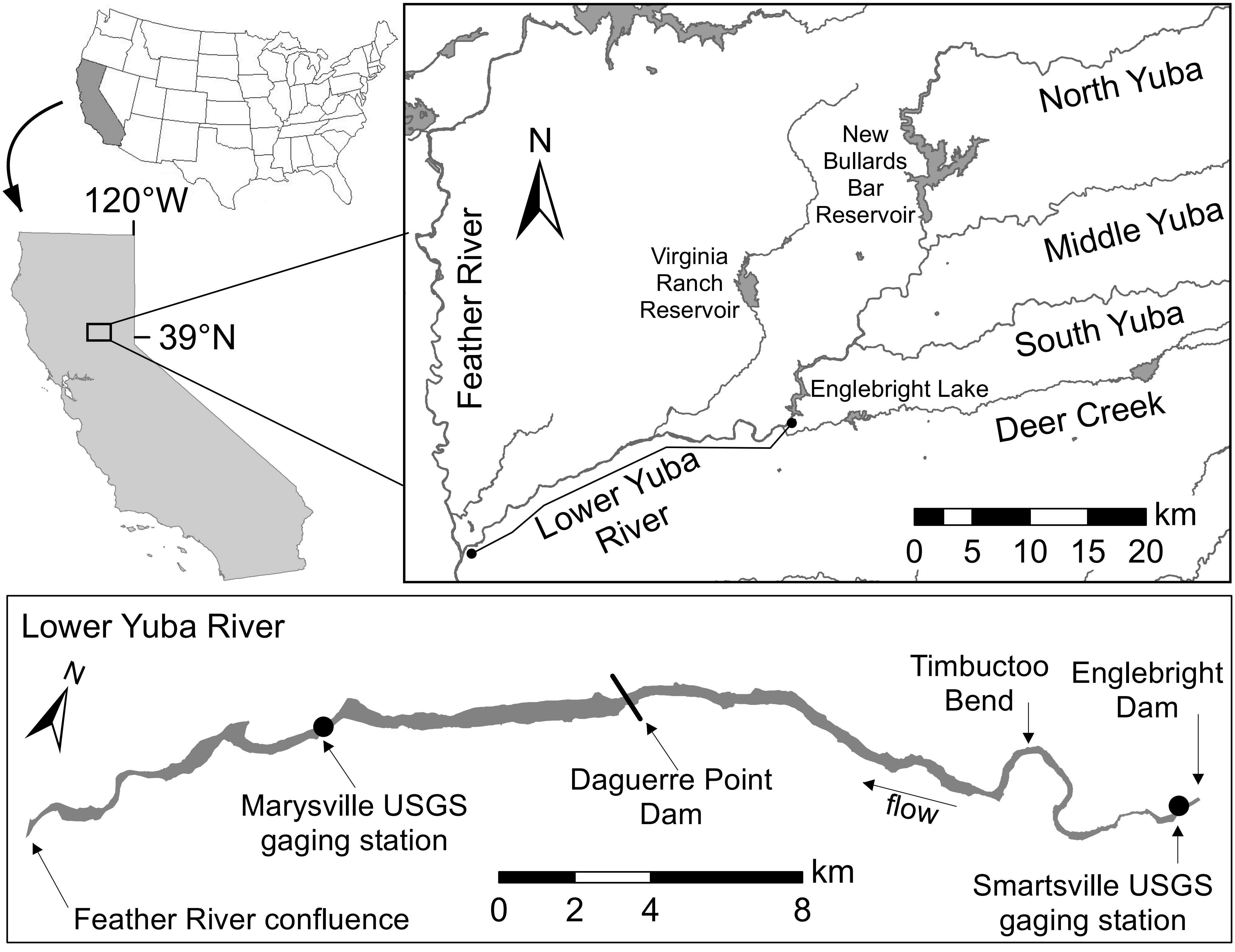

120°W
39°N
N
North Yuba
New
Bullards
Bar
Reservoir
Middle Yuba
Virginia
Ranch
Reservoir
Feather River
South Yuba
Englebright Lake
Deer Creek
Lower Yuba
River
km
0 5 10 15 20
Lower Yuba River
N
Timbuctoo
Bend
Englebright
Dam
Marysville USGS
gaging station
Daguerre Point
Dam
flow
Smartsville USGS
gaging station
Feather River confluence
km
0 2 4 8

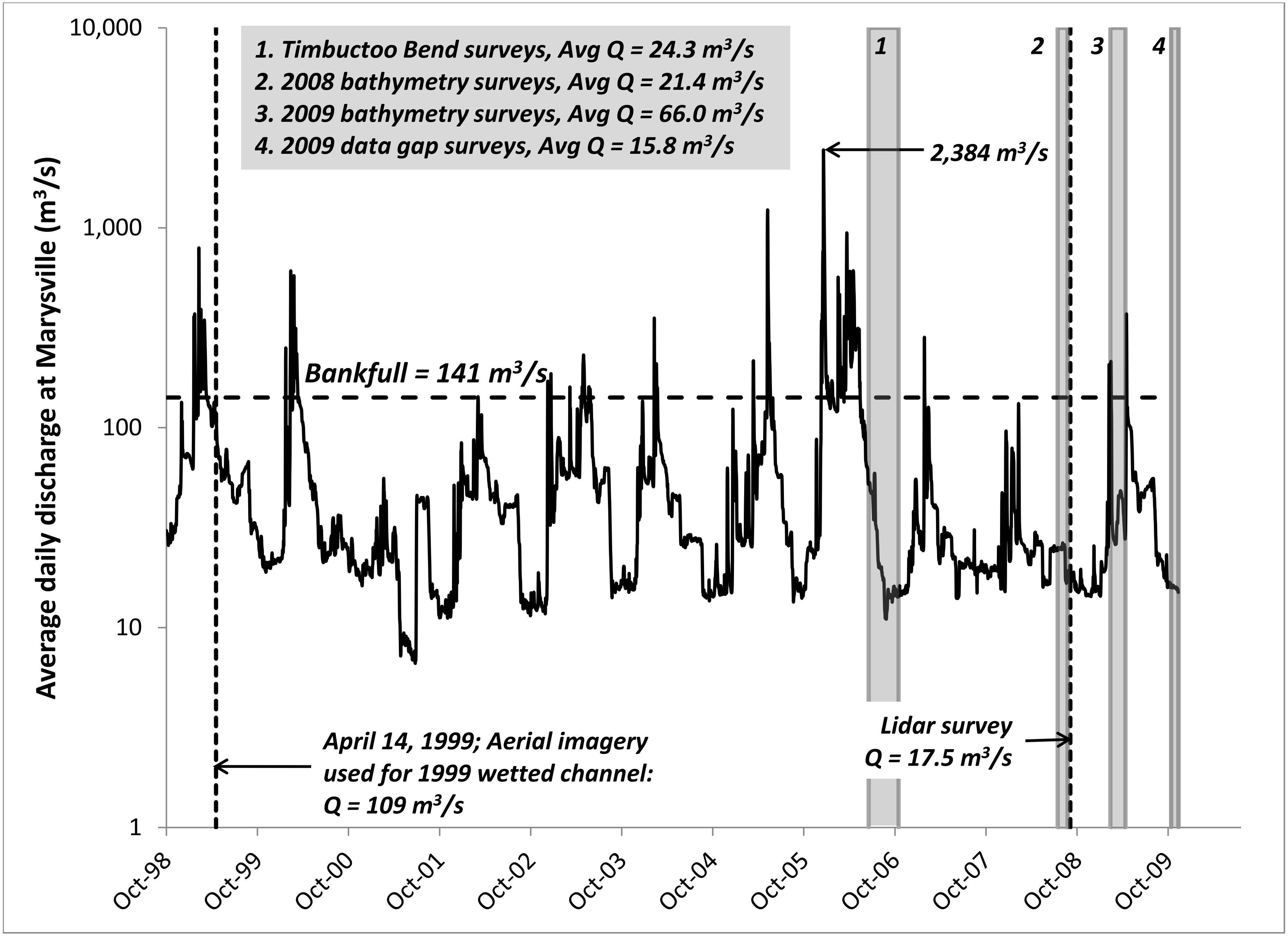

1. Timbuctoo Bend surveys, Avg Q = 24.3 m3/s
2. 2008 bathymetry surveys, Avg Q = 21.4 m3/s
3. 2009 bathymetry surveys, Avg Q = 66.0 m3/s
4. 2009 data gap surveys, Avg Q = 15.8 m3/s
2,384 m3/s
Bankfull = 141 m3/s
1
2
3
4
April 14, 1999; Aerial imagery used for 1999 wetted channel: Q = 109 m3/s
Lidar survey Q = 17.5 m3/s
Average daily discharge at Marysville (m3/s)
10,000
1,000
100
10
1
Oct-98
Oct-99
Oct-00
Oct-01
Oct-02
Oct-03
Oct-04
Oct-05
Oct-06
Oct-07
Oct-08
Oct-09

Topographic change detection workflow

a. Create a uniform {x,y} point grid with 0.3 m point spacing.

b. Elevate the 0.3 m point grid using the topographic data for each map to create oversampled topographic point datasets for $\{x,y,z\}_{time1}$ and $\{x,y,z\}_{time2}$ that capture all available topographic information in the source DEMs.

c. For each 0.3 m {x,y,z} topographic dataset, create a raster of standard deviation (SD) of point elevation with a 1.5 x 1.5 m cell size (yielding 25 points per cell in the statistical computation).

d. Apply the appropriate survey and instrument error (SIE) empirical equation from Heritage *et al.* (2009) to the SD rasters to obtain the SIE raster for each topographic map.

e. Produce a Level of Detection (LoD) grid that combines the two SIE rasters into a single error raster using the t-value for 95 % confidence (1.96) and the statistical equation for error propagation given by:

$$LoD = t\sqrt{(SIE_{time1})^2 + (SIE_{time2})^2}$$

f. Create the raw DoD raster with a 1.5 x 1.5 m cell size.

g. Create separate deposition and erosion rasters using the “Con” function in the ArcGIS raster calculator.

h. Remove the LoD from each raster by subtracting it from the deposition-only raw DoD and adding it to the erosion-only raw DoD.

Delineation of topographic change processes workflow

a. Create a DoD raster using the workflow presented in Figure 3.

b. For the DoD raster, use the “Con” function in the ArcGIS raster calculator to create separate presence/absence rasters of scour, fill, and no detectable change. Convert the rasters into polygons.

c. Split the study area polygon into four regions based on the bankfull wetted areas of each survey period. The regions include (1) not wetted at either time, (2) wetted for both times, (3) wetted during first survey, but not the second, and (4) wetted during the second survey, but not the first.

d. Based on expert judgment and available data, additionally split the study area polygon by other factors controlling topographic change processes, such as morphological units, presence/absence of vegetation, sediment facies, etc.

e. With these segregated polygon maps (i.e. scour-fill, wetted regions, and other relevant geomorphic controls) as inputs, use the “identity” function in ArcGIS to identify the suite of like polygons that exhibit the same set of segregation characteristics.

f. Assign appropriate nomenclature for each unique suite.

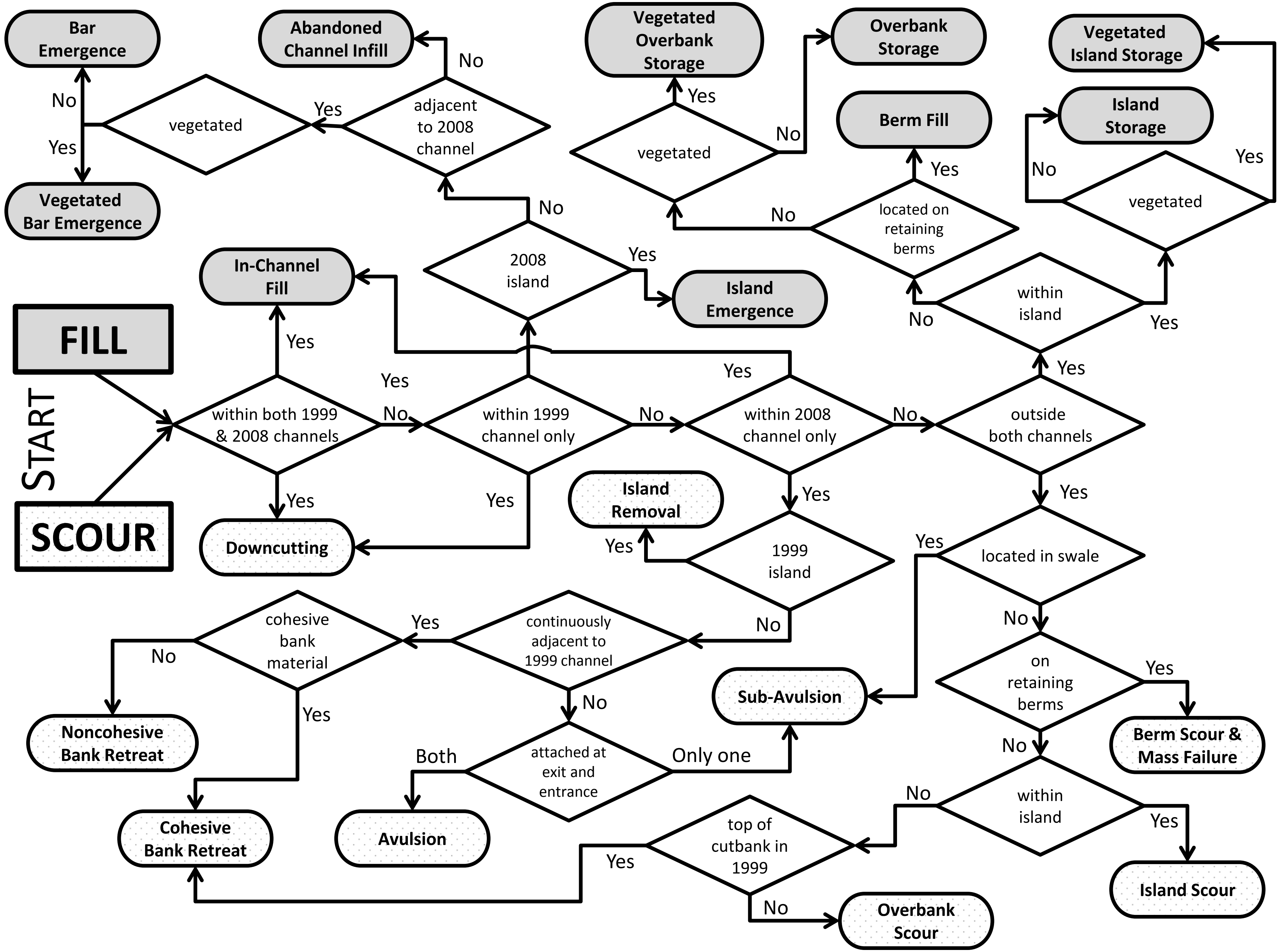

START
FILL
SCOUR
within both 1999 & 2008 channels
within 1999 channel only
within 2008 channel only
outside both channels
In-Channel Fill
Downcutting
2008 island
Island Emergence
adjacent to 2008 channel
Abandoned Channel Infill
vegetated
Bar Emergence
Vegetated Bar Emergence
Vegetated Overbank Storage
Overbank Storage
Berm Fill
located on retaining berms
within island
Vegetated Island Storage
Island Storage
Island Removal
1999 island
continuously adjacent to 1999 channel
cohesive bank material
Noncohesive Bank Retreat
Cohesive Bank Retreat
attached at exit and entrance
Both
Only one
Avulsion
Sub-Avulsion
located in swale
on retaining berms
Berm Scour & Mass Failure
Island Scour
top of cutbank in 1999
Overbank Scour
Yes
No

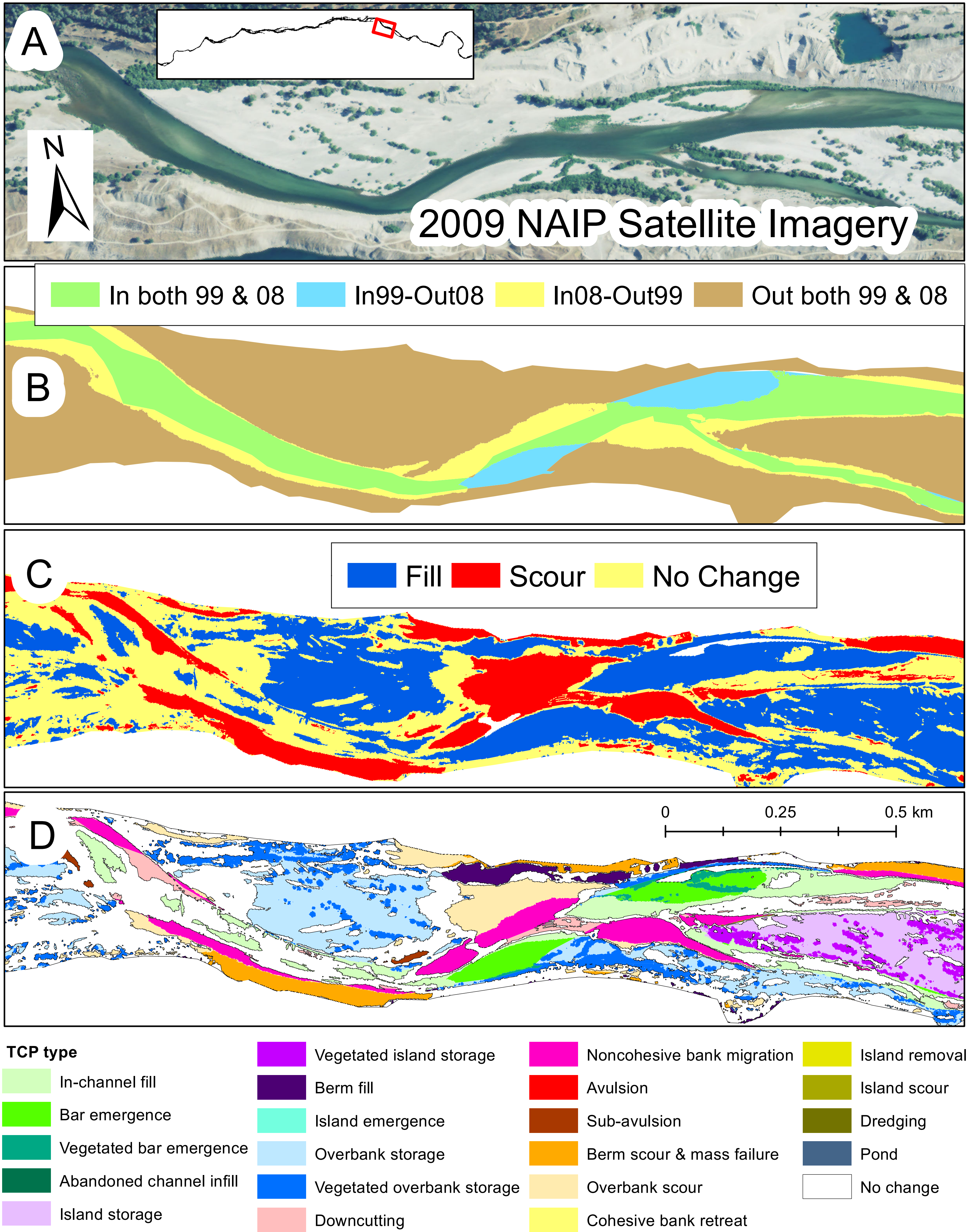
A
2009 NAIP Satellite Imagery
N
B
In both 99 & 08
In99-Out08
In08-Out99
Out both 99 & 08
C
Fill
Scour
No Change
D
0
0.25
0.5 km
TCP type
In-channel fill
Bar emergence
Vegetated bar emergence
Abandoned channel infill
Island storage
Vegetated island storage
Berm fill
Island emergence
Overbank storage
Vegetated overbank storage
Downcutting
Noncohesive bank migration
Avulsion
Sub-avulsion
Berm scour & mass failure
Overbank scour
Cohesive bank retreat
Island removal
Island scour
Dredging
Pond
No change

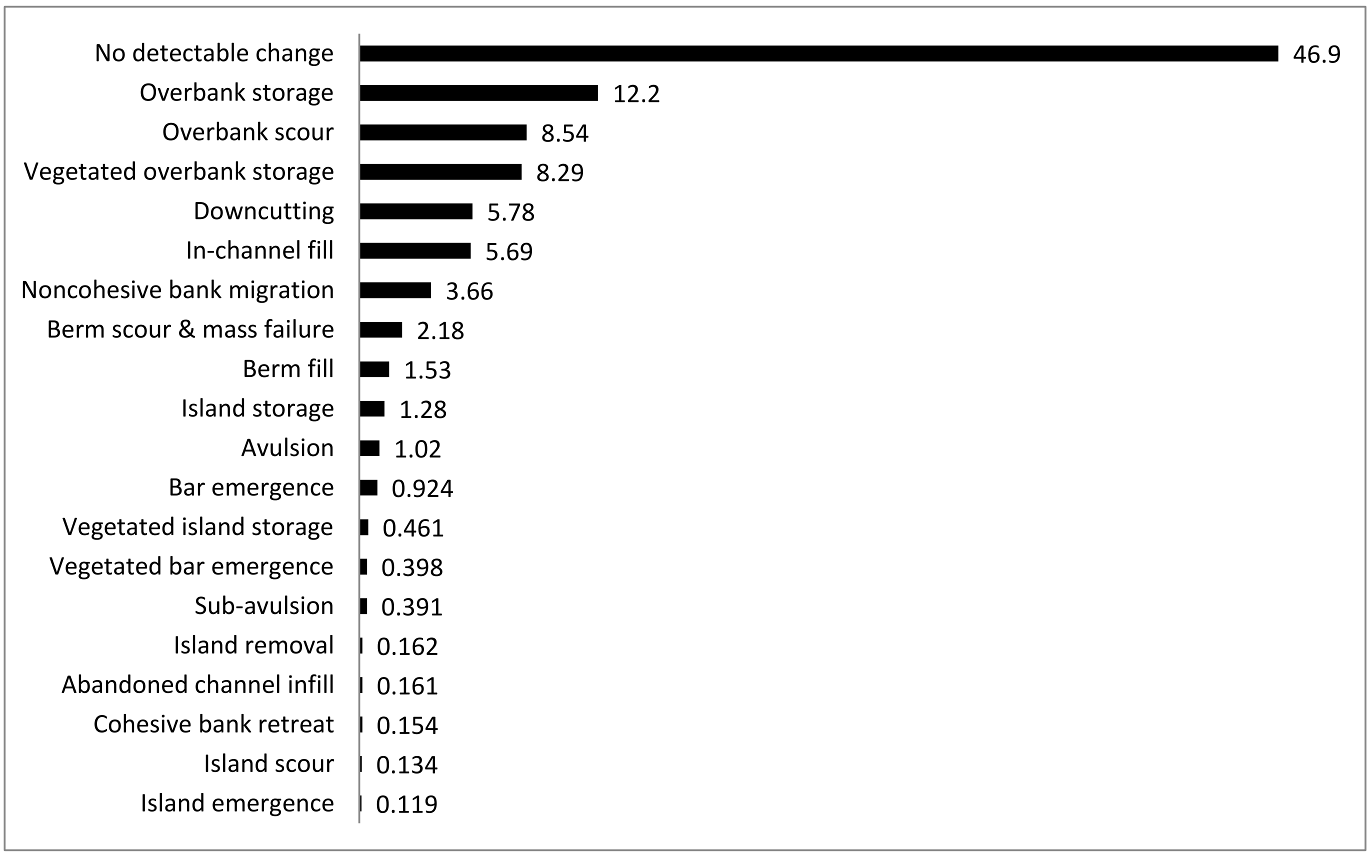

No detectable change
46.9
Overbank storage
12.2
Overbank scour
8.54
Vegetated overbank storage
8.29
Downcutting
5.78
In-channel fill
5.69
Noncohesive bank migration
3.66
Berm scour & mass failure
2.18
Berm fill
1.53
Island storage
1.28
Avulsion
1.02
Bar emergence
0.924
Vegetated island storage
0.461
Vegetated bar emergence
0.398
Sub-avulsion
0.391
Island removal
0.162
Abandoned channel infill
0.161
Cohesive bank retreat
0.154
Island scour
0.134
Island emergence
0.119

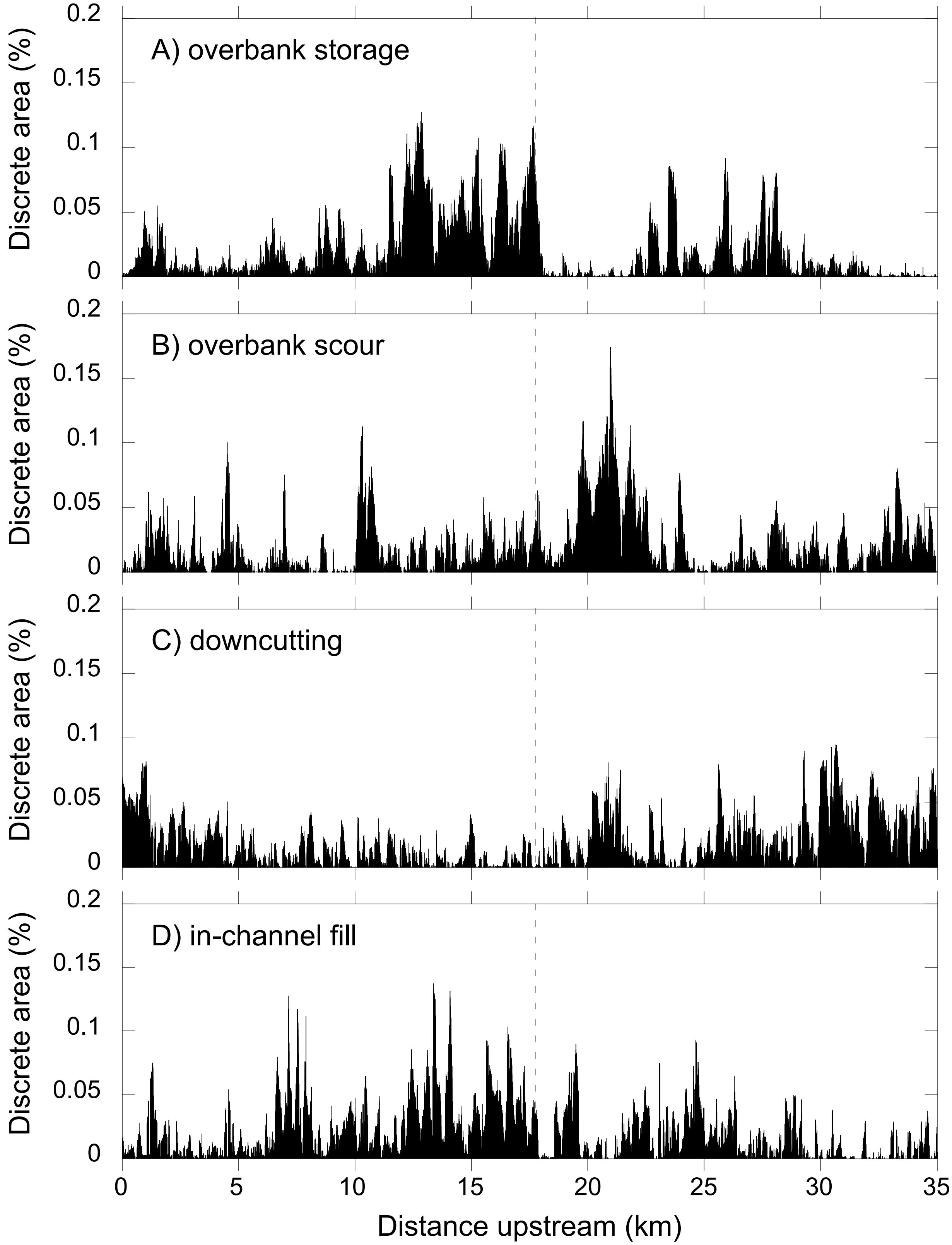

A) overbank storage
B) overbank scour
C) downcutting
D) in-channel fill
Discrete area (%)
0
0.05
0.1
0.15
0.2
0
5
10
15
20
25
30
35
Distance upstream (km)

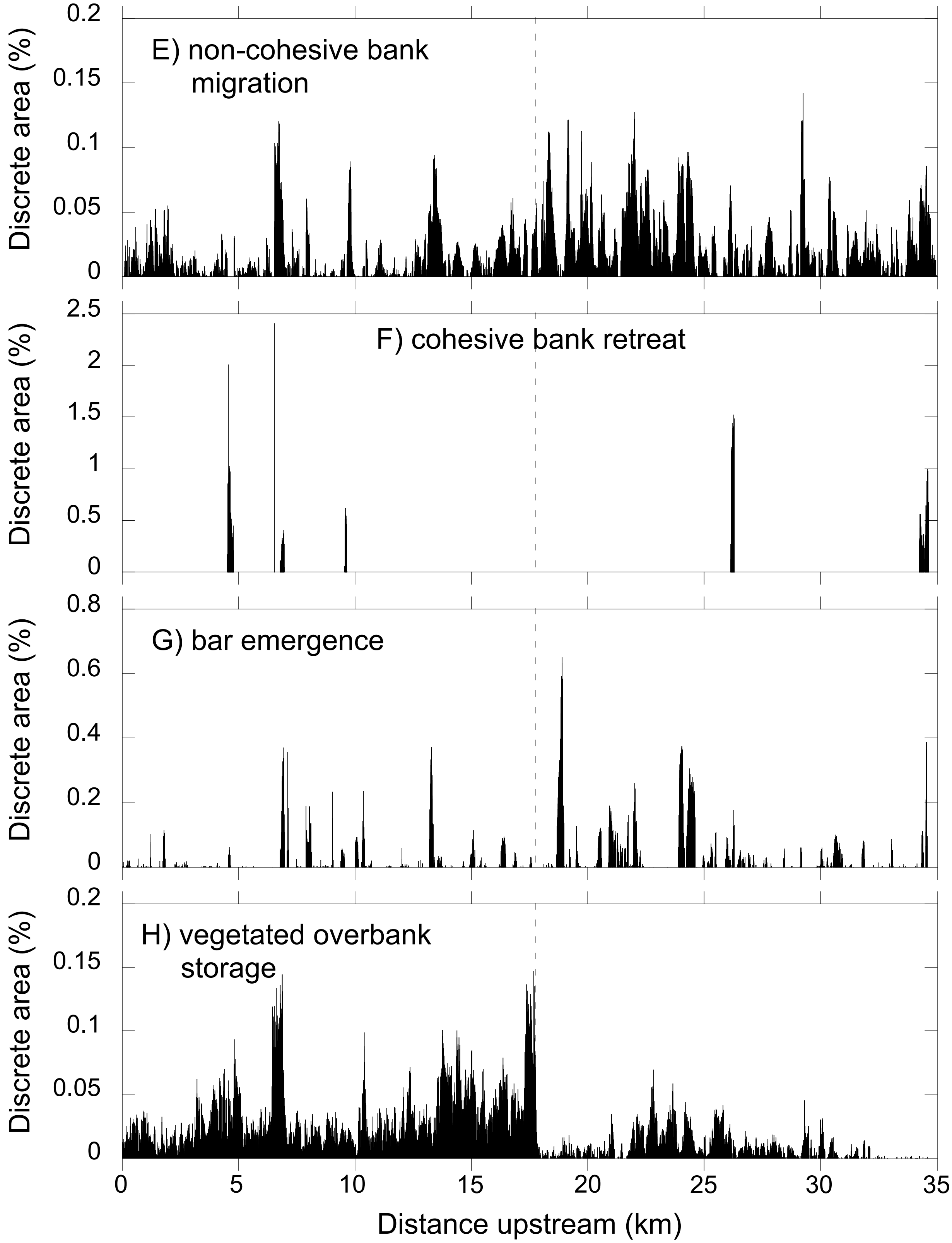

E) non-cohesive bank migration
F) cohesive bank retreat
G) bar emergence
H) vegetated overbank storage
Discrete area (%)
Distance upstream (km)
0
0.05
0.1
0.15
0.2
0.5
1
1.5
2
2.5
0.2
0.4
0.6
0.8
5
10
15
20
25
30
35

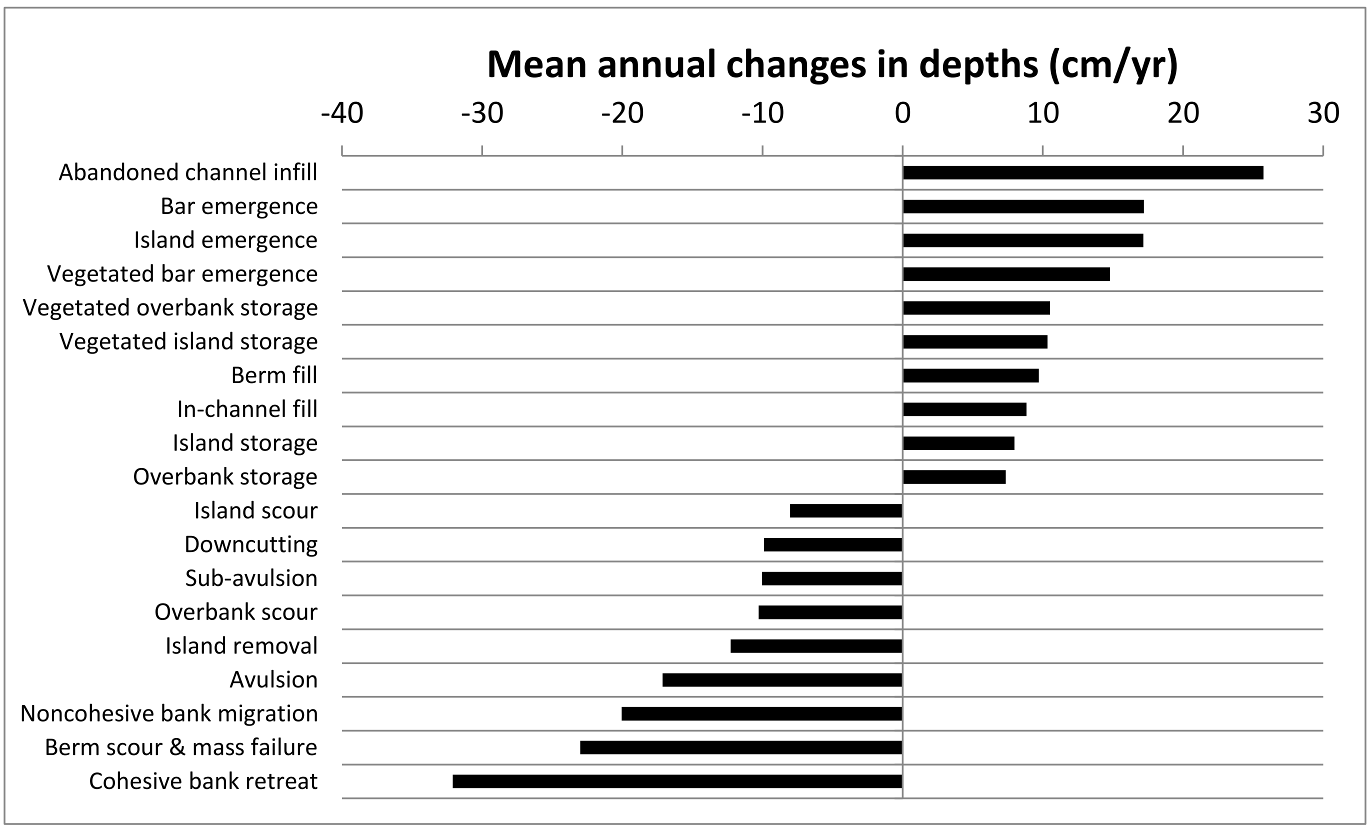
Mean annual changes in depths (cm/yr)
-40
-30
-20
-10
0
10
20
30
Abandoned channel infill
Bar emergence
Island emergence
Vegetated bar emergence
Vegetated overbank storage
Vegetated island storage
Berm fill
In-channel fill
Island storage
Overbank storage
Island scour
Downcutting
Sub-avulsion
Overbank scour
Island removal
Avulsion
Noncohesive bank migration
Berm scour & mass failure
Cohesive bank retreat

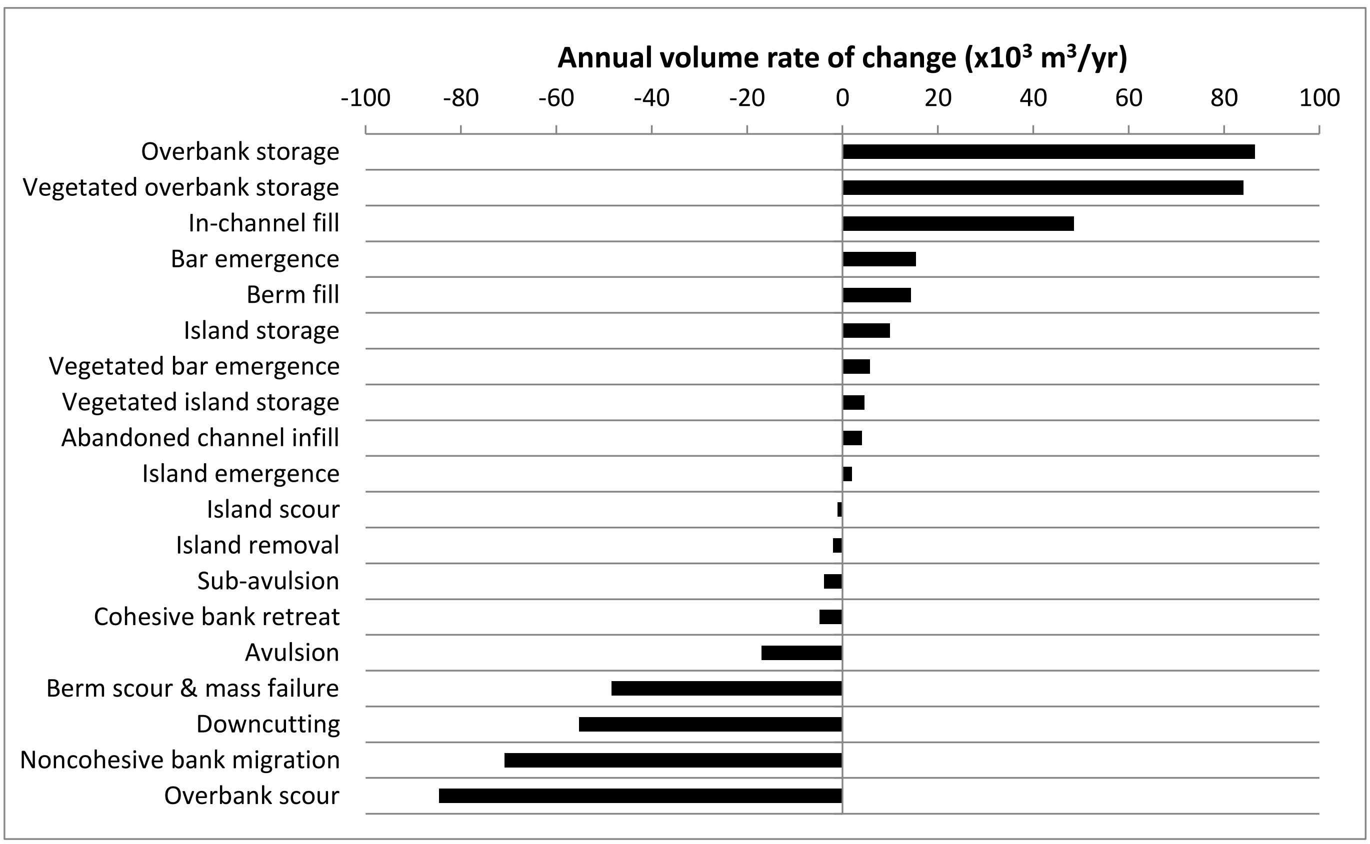
Annual volume rate of change (x10³ m³/yr)
-100
-80
-60
-40
-20
0
20
40
60
80
100
Overbank storage
Vegetated overbank storage
In-channel fill
Bar emergence
Berm fill
Island storage
Vegetated bar emergence
Vegetated island storage
Abandoned channel infill
Island emergence
Island scour
Island removal
Sub-avulsion
Cohesive bank retreat
Avulsion
Berm scour & mass failure
Downcutting
Noncohesive bank migration
Overbank scour

LYR DEM differences: areal divisions

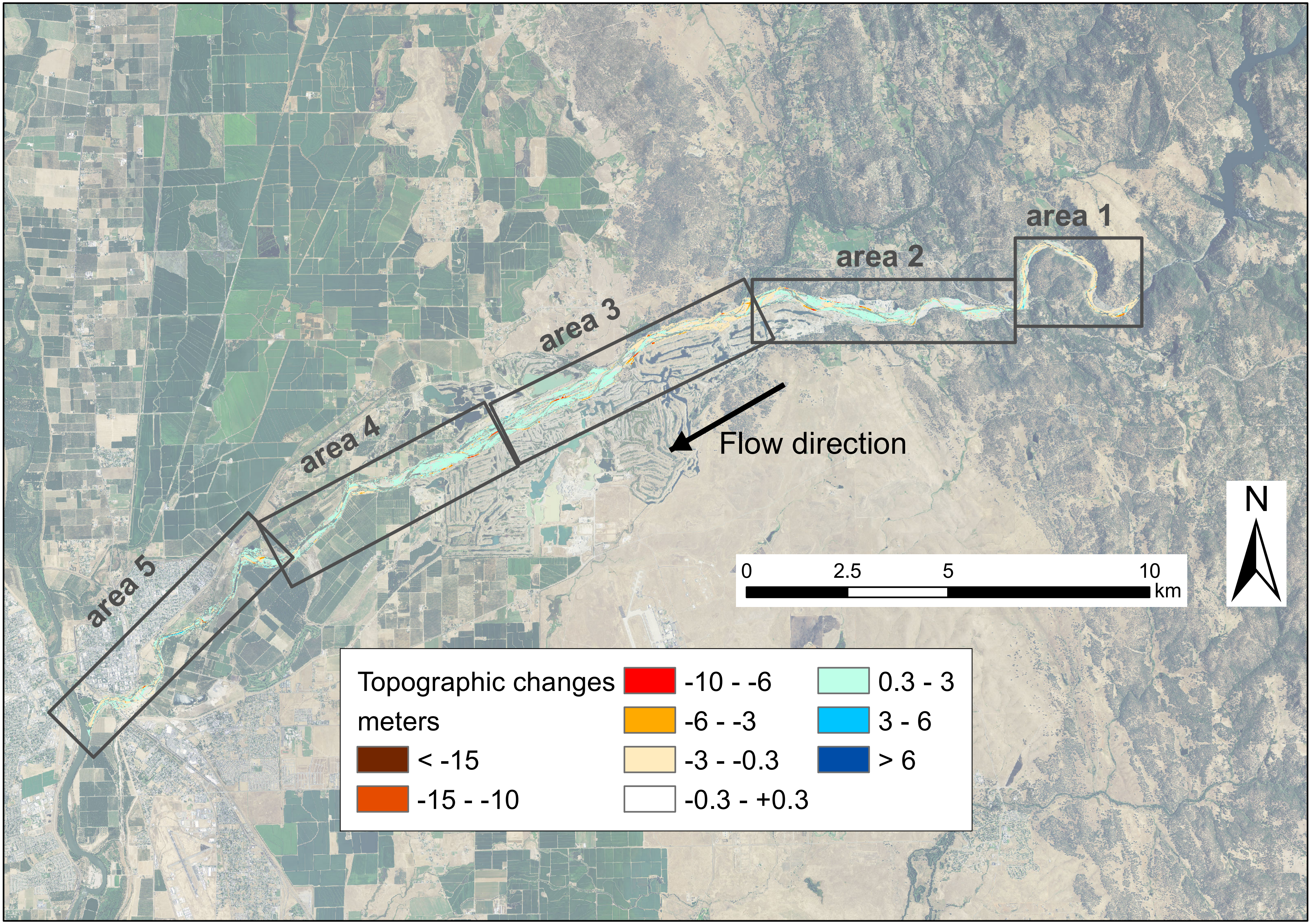

LYR DEM differences: area 1

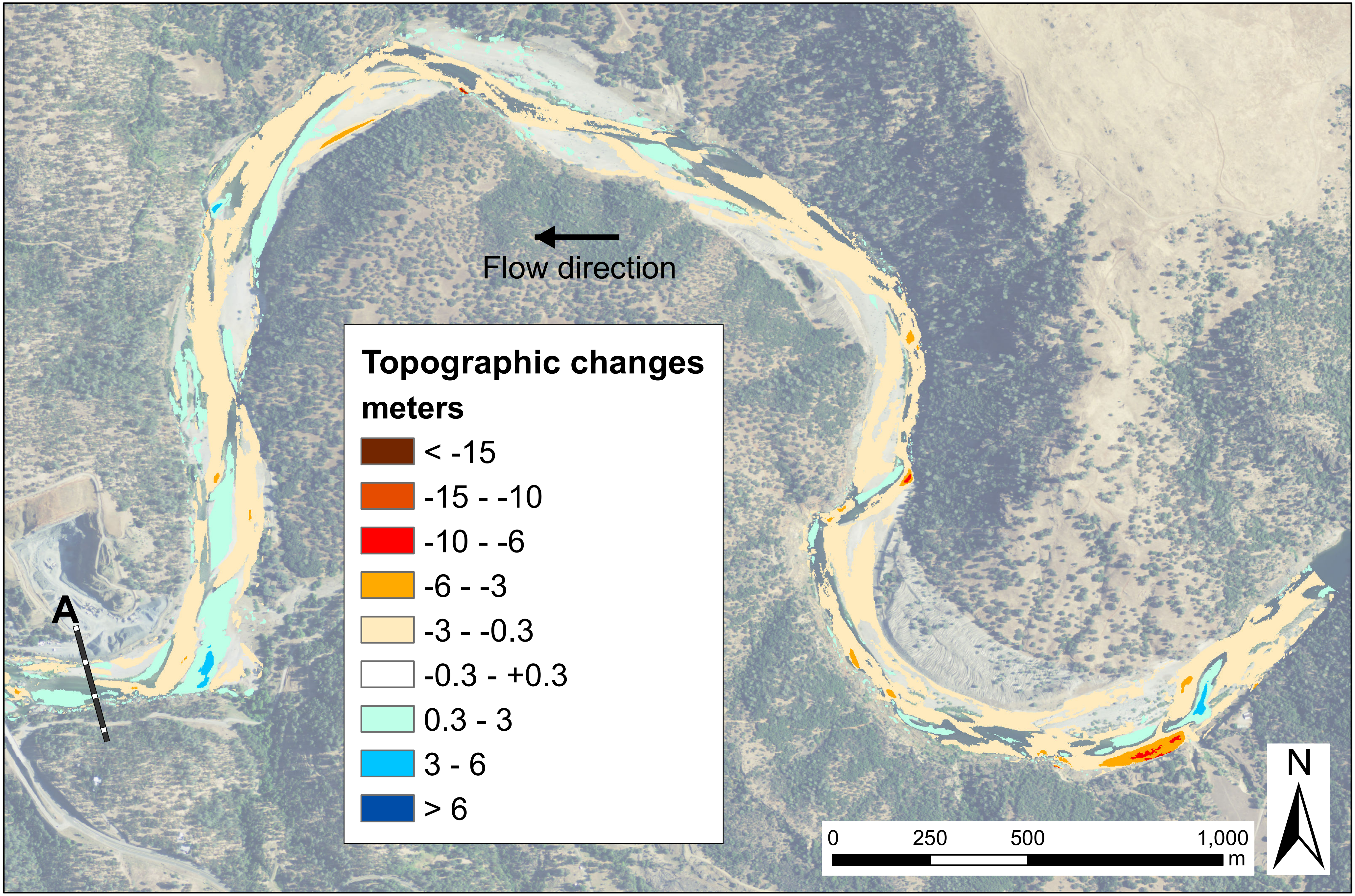

LYR DEM differences: area 2

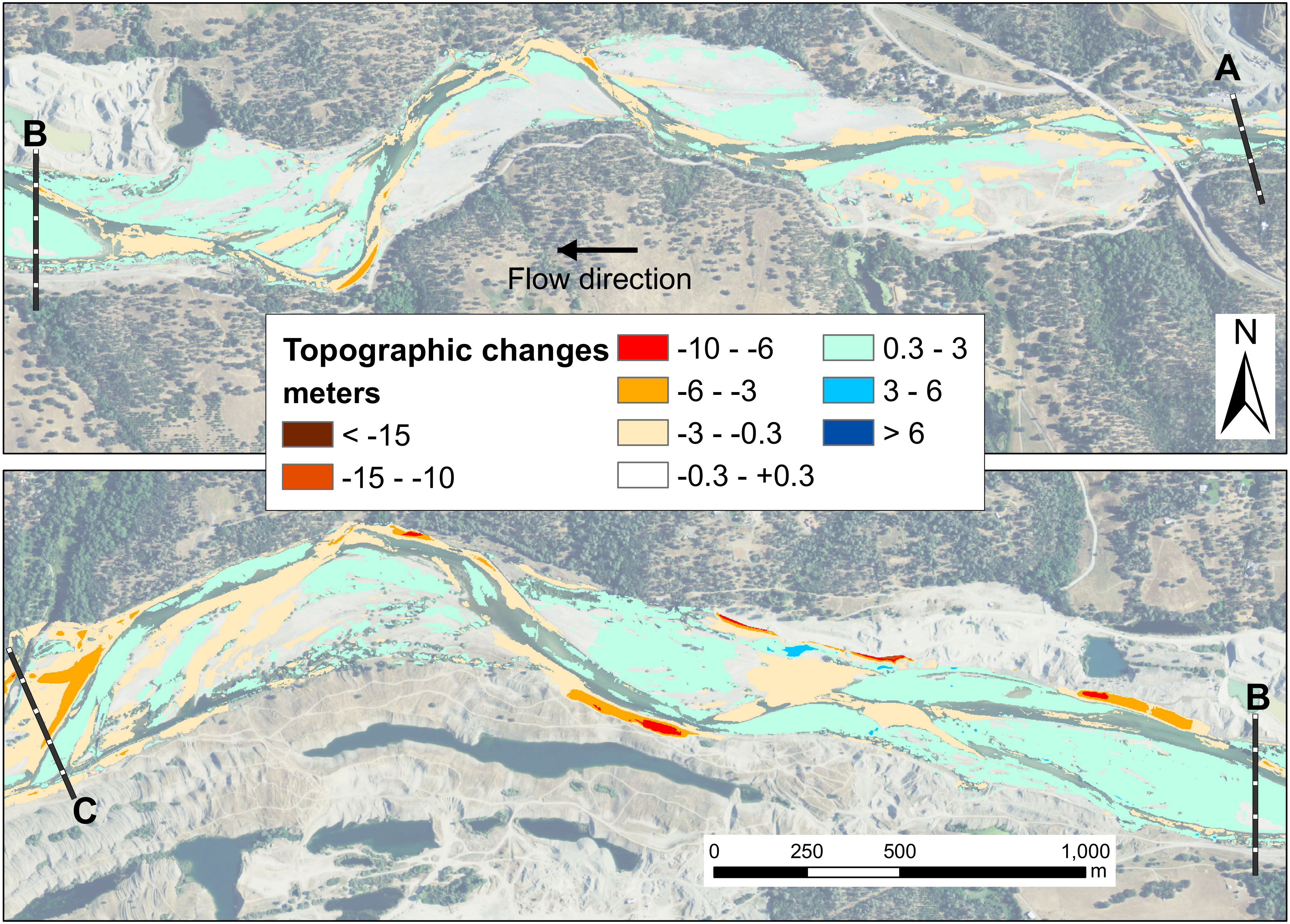

LYR DEM differences: area 3

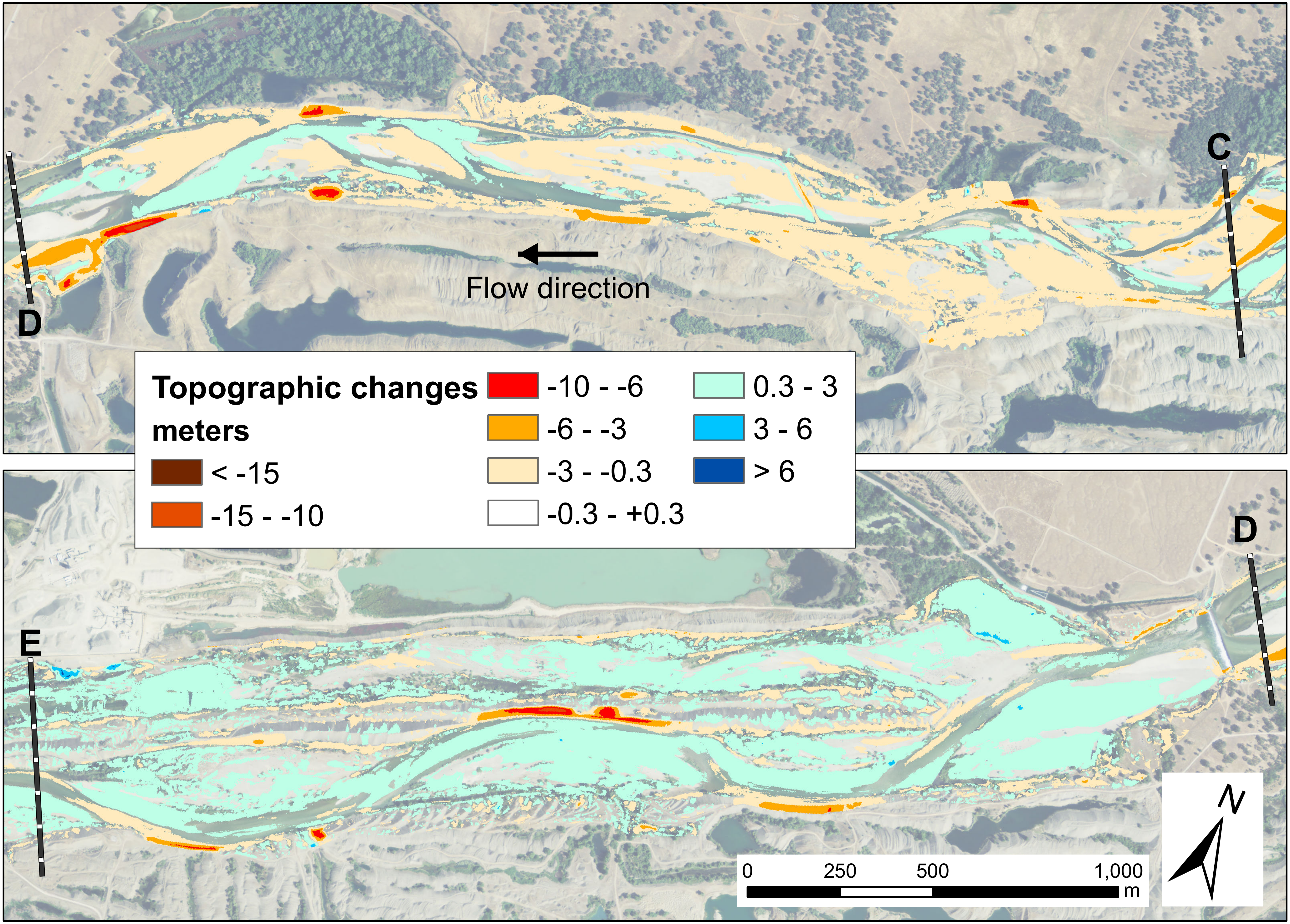

LYR DEM differences: area 4

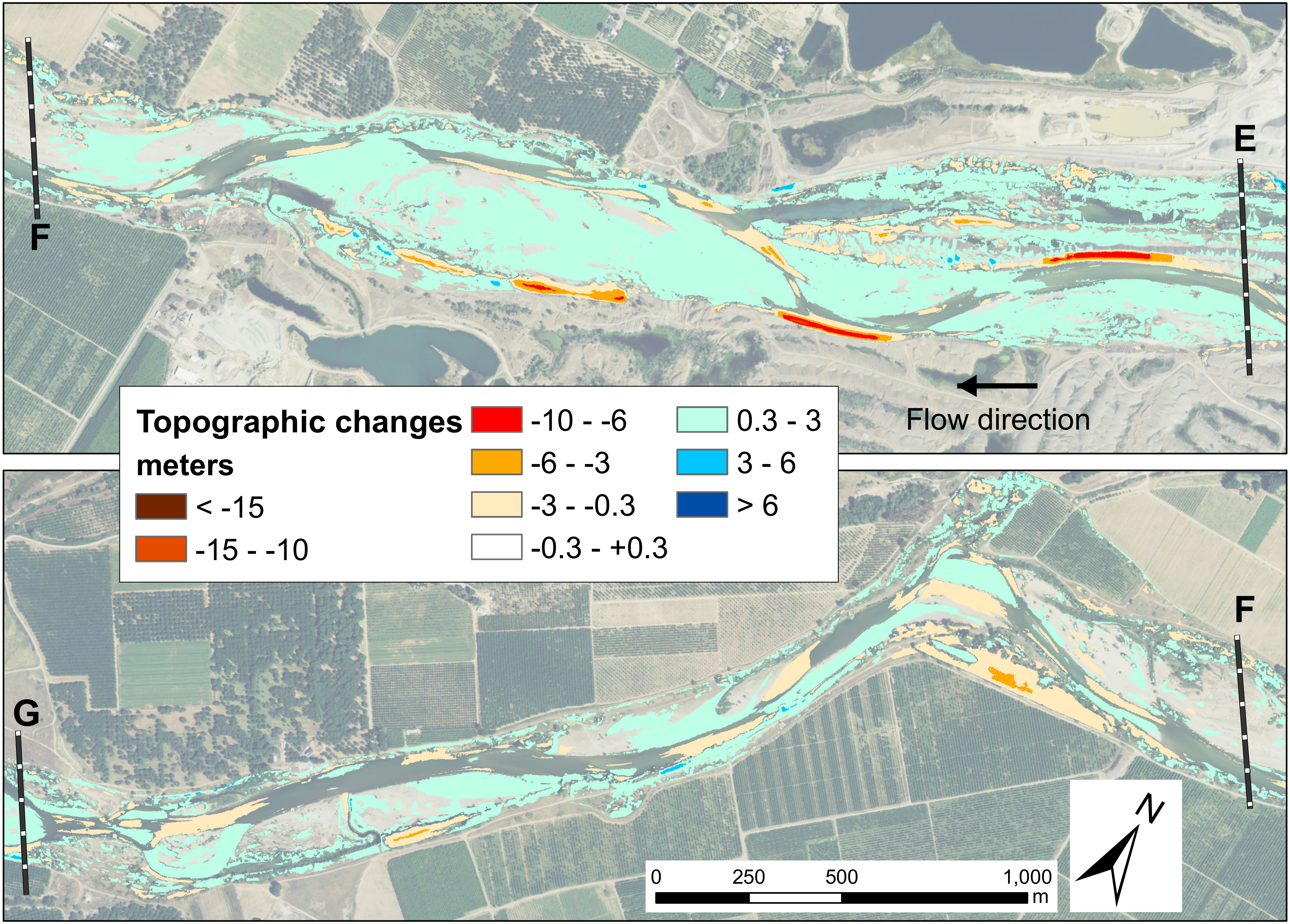

LYR DEM differences: area 5

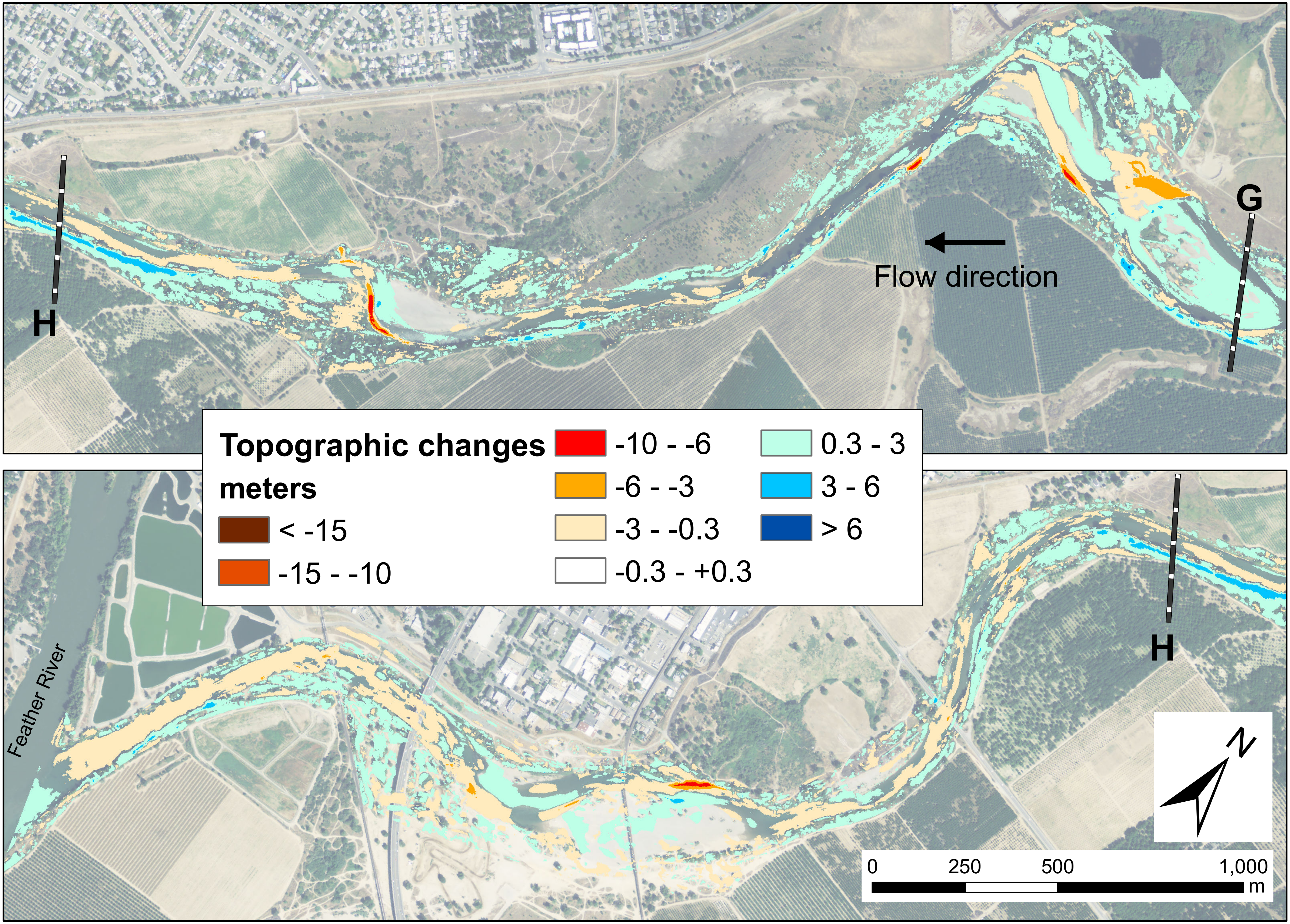

LYR TCP: areal divisions

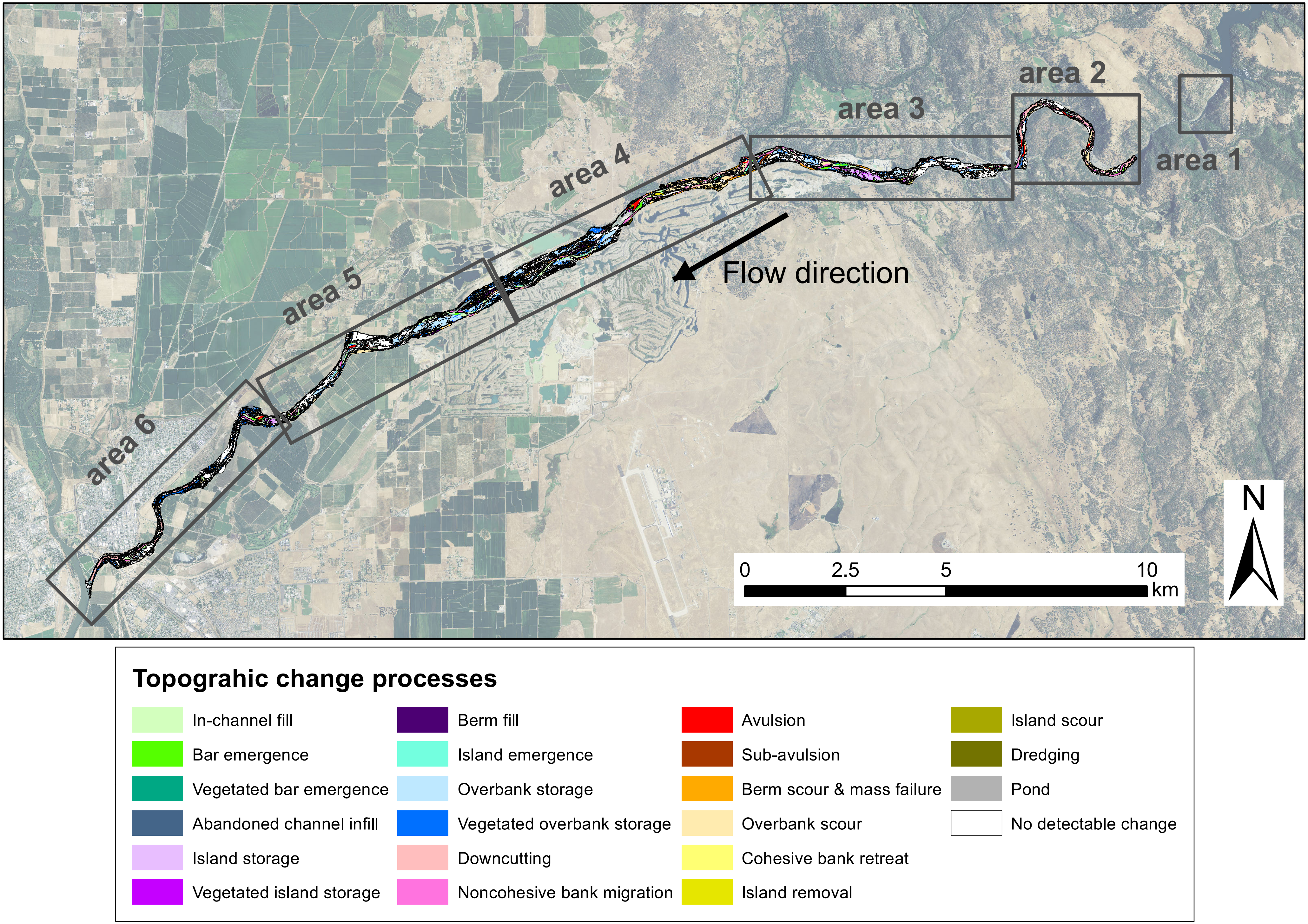

LYR TCP: area 2

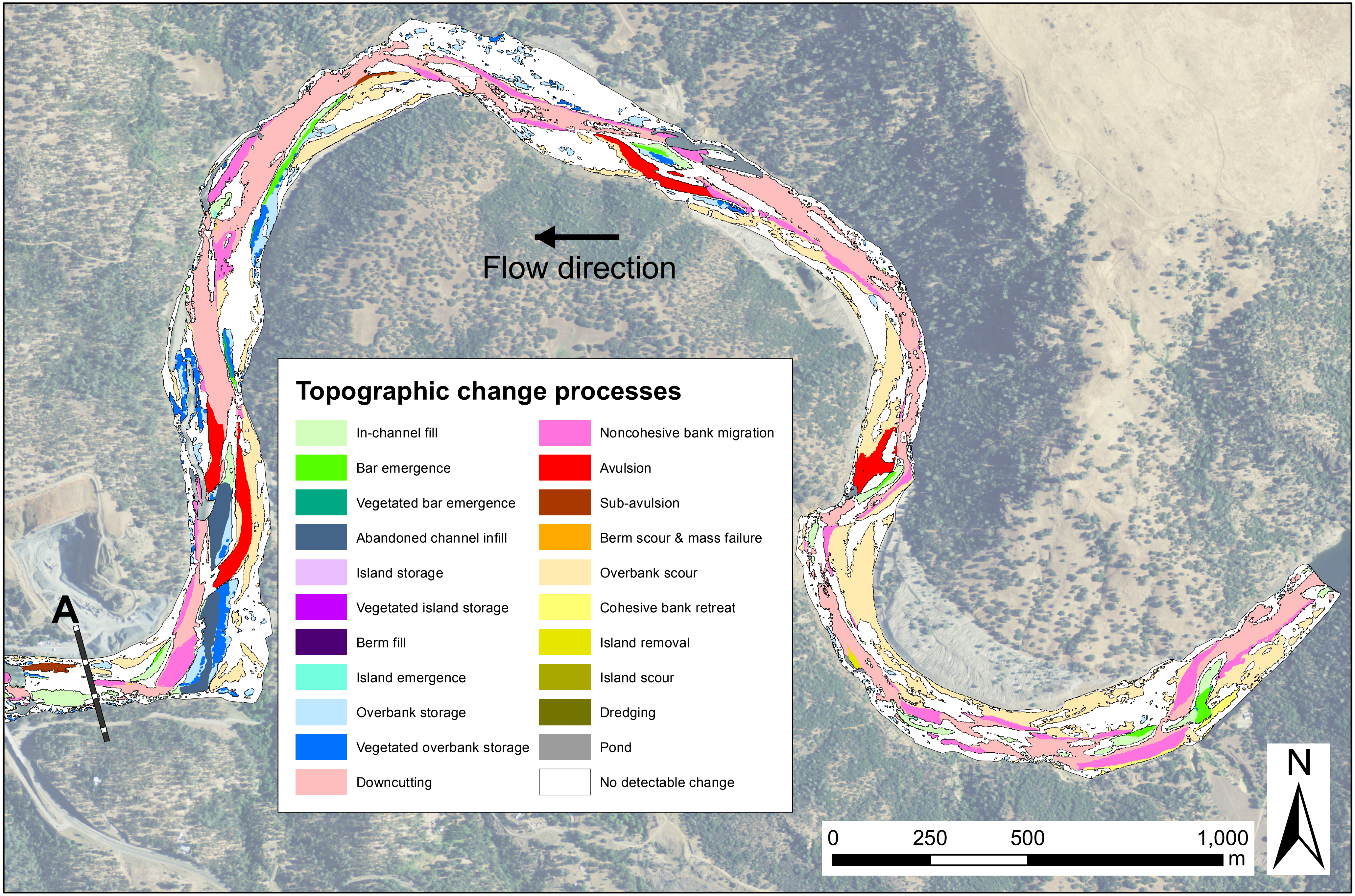

LYR TCP: area 3

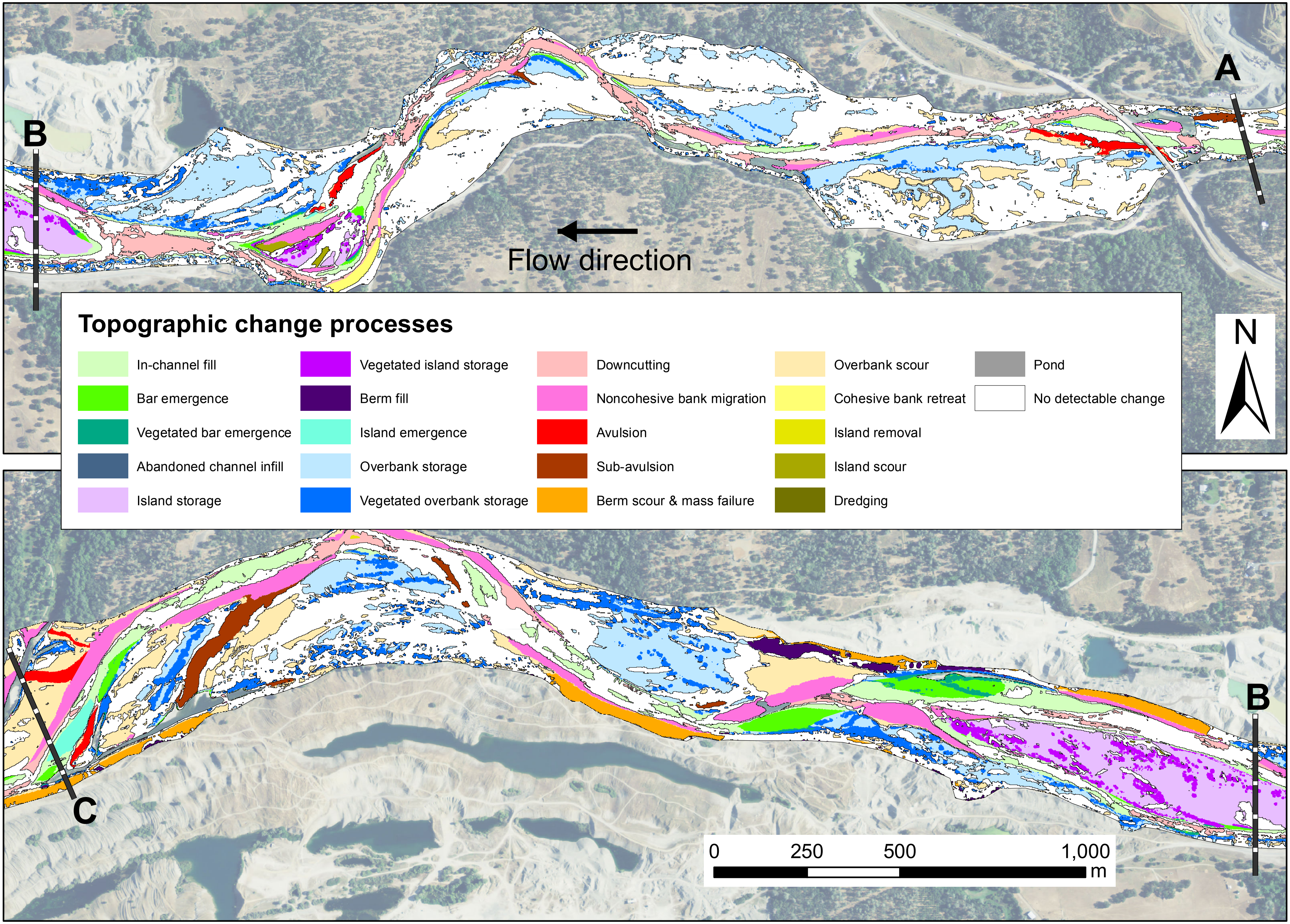

LYR TCP: area 4

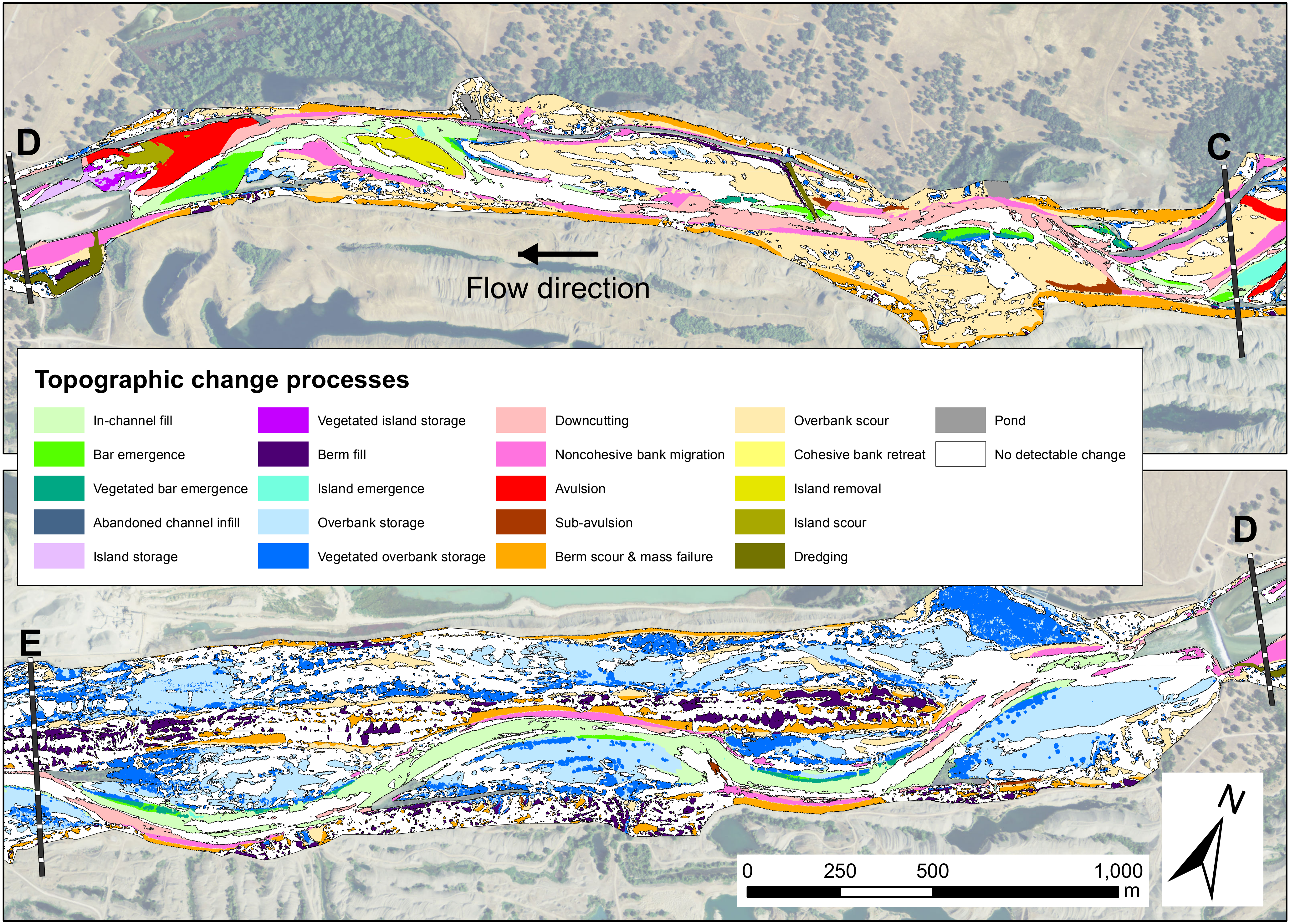

LYR TCP: area 5

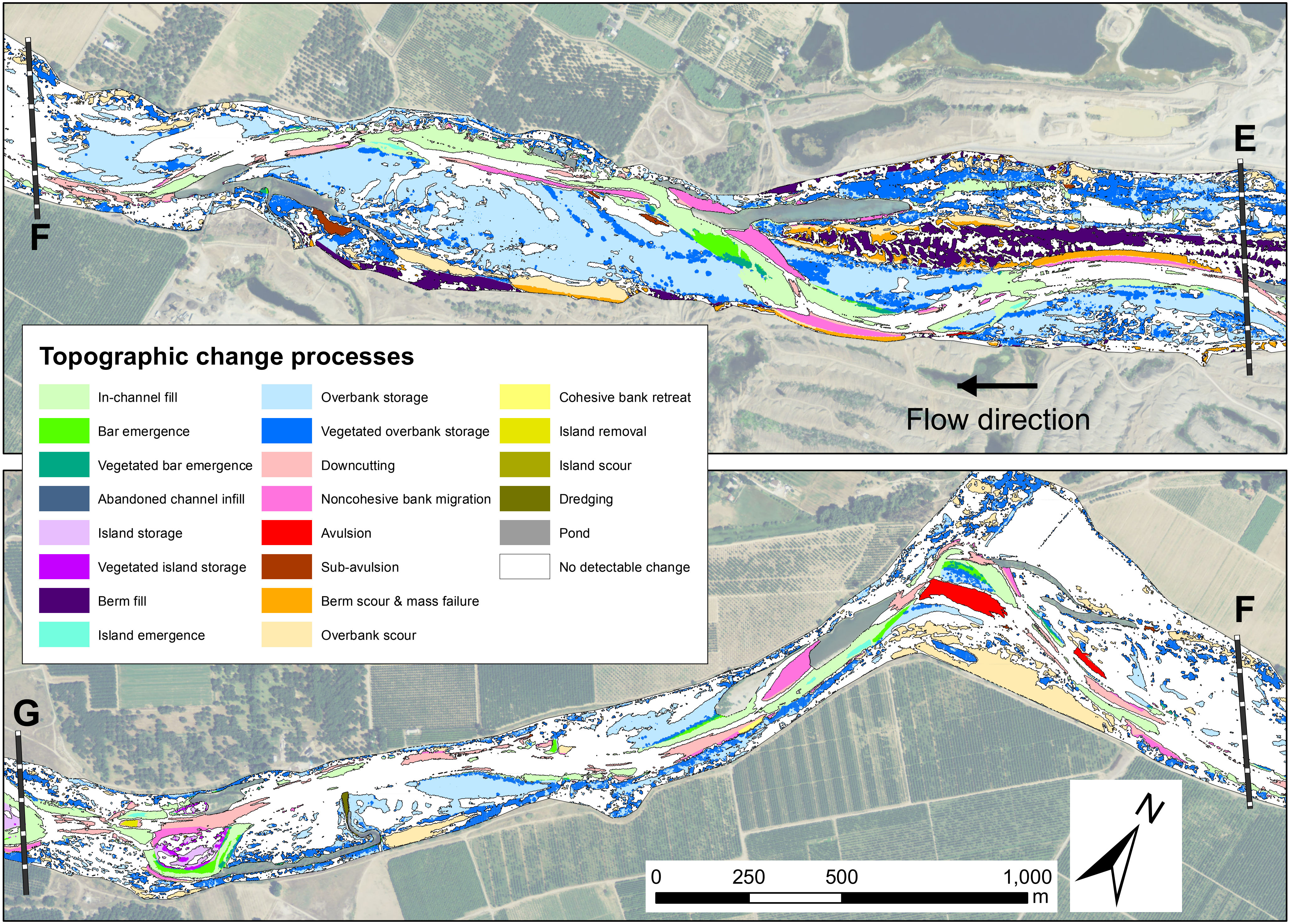

LYR TCP: area 6

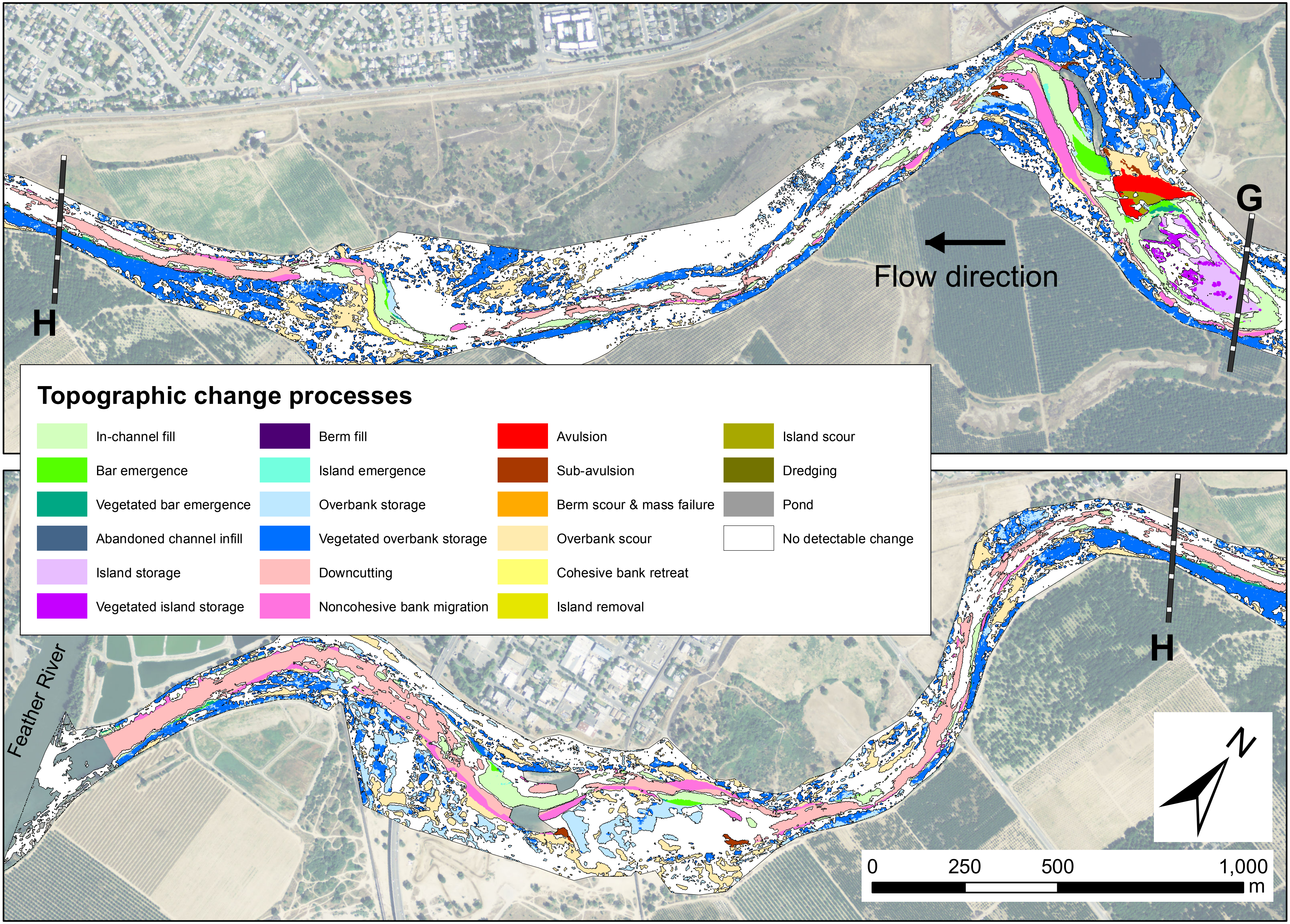

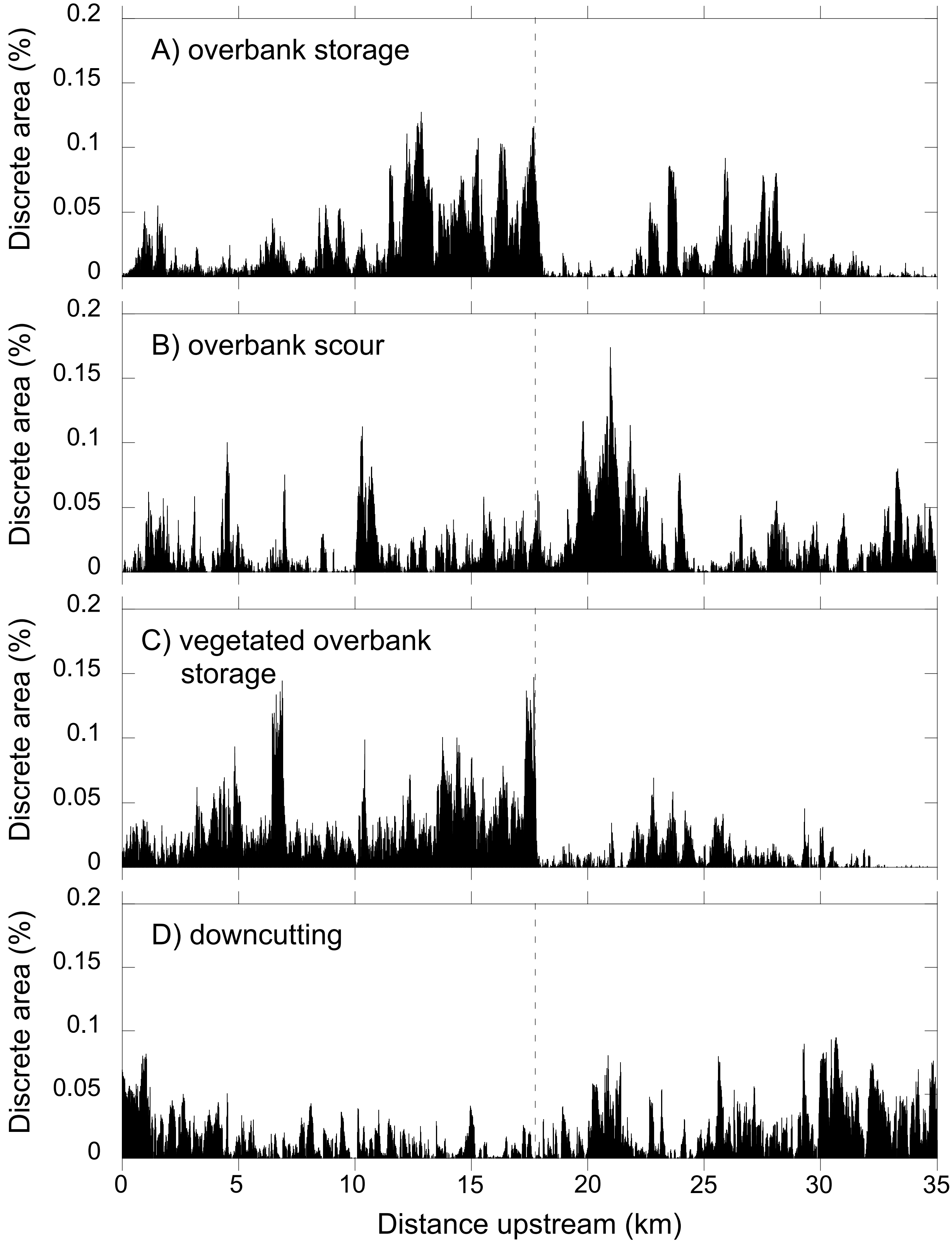
A) overbank storage
B) overbank scour
C) vegetated overbank storage
D) downcutting
Discrete area (%)
0
0.05
0.1
0.15
0.2
0
5
10
15
20
25
30
35
Distance upstream (km)

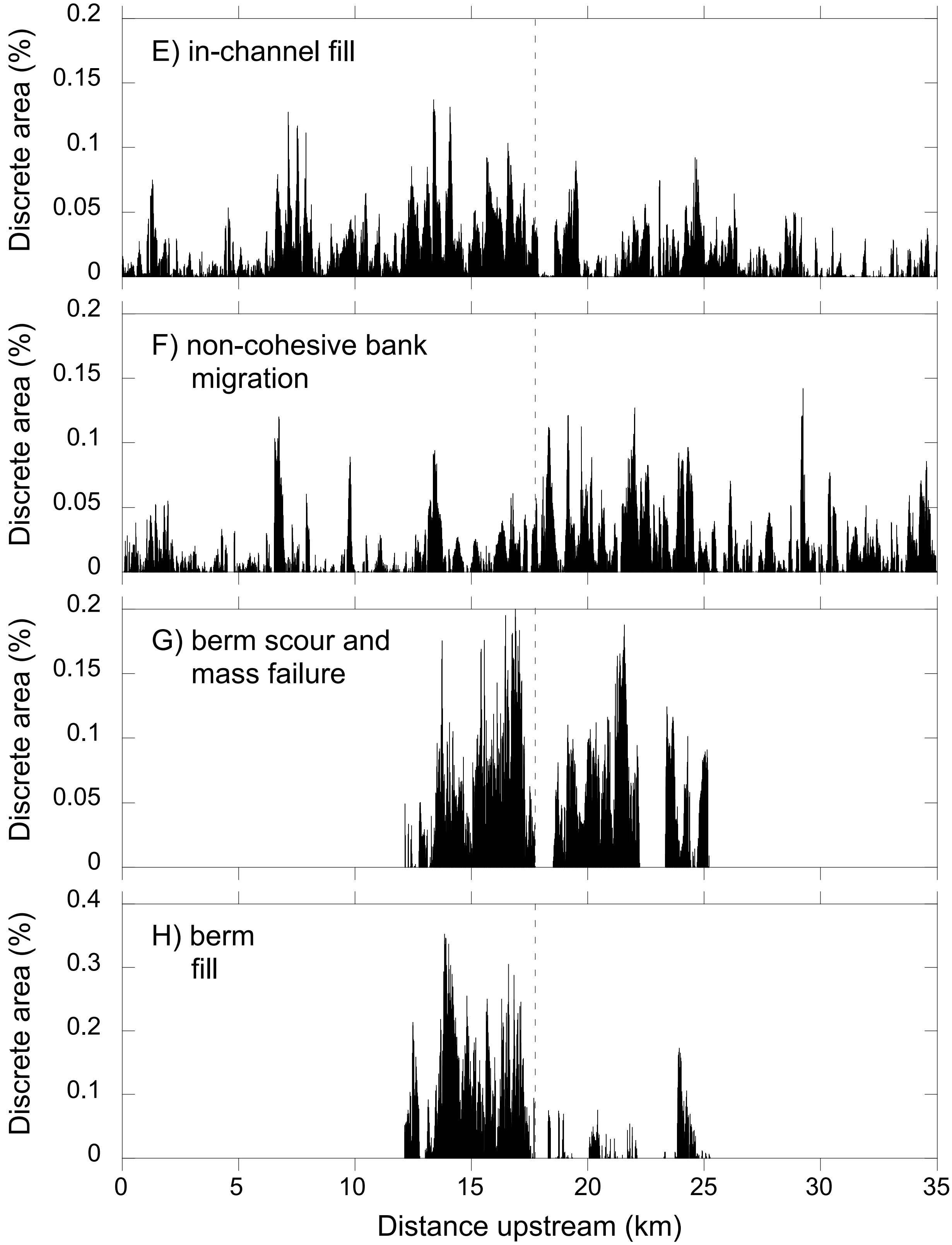
E) in-channel fill
F) non-cohesive bank migration
G) berm scour and mass failure
H) berm fill
Discrete area (%)
0
0.05
0.1
0.15
0.2
0.3
0.4
0
5
10
15
20
25
30
35
Distance upstream (km)

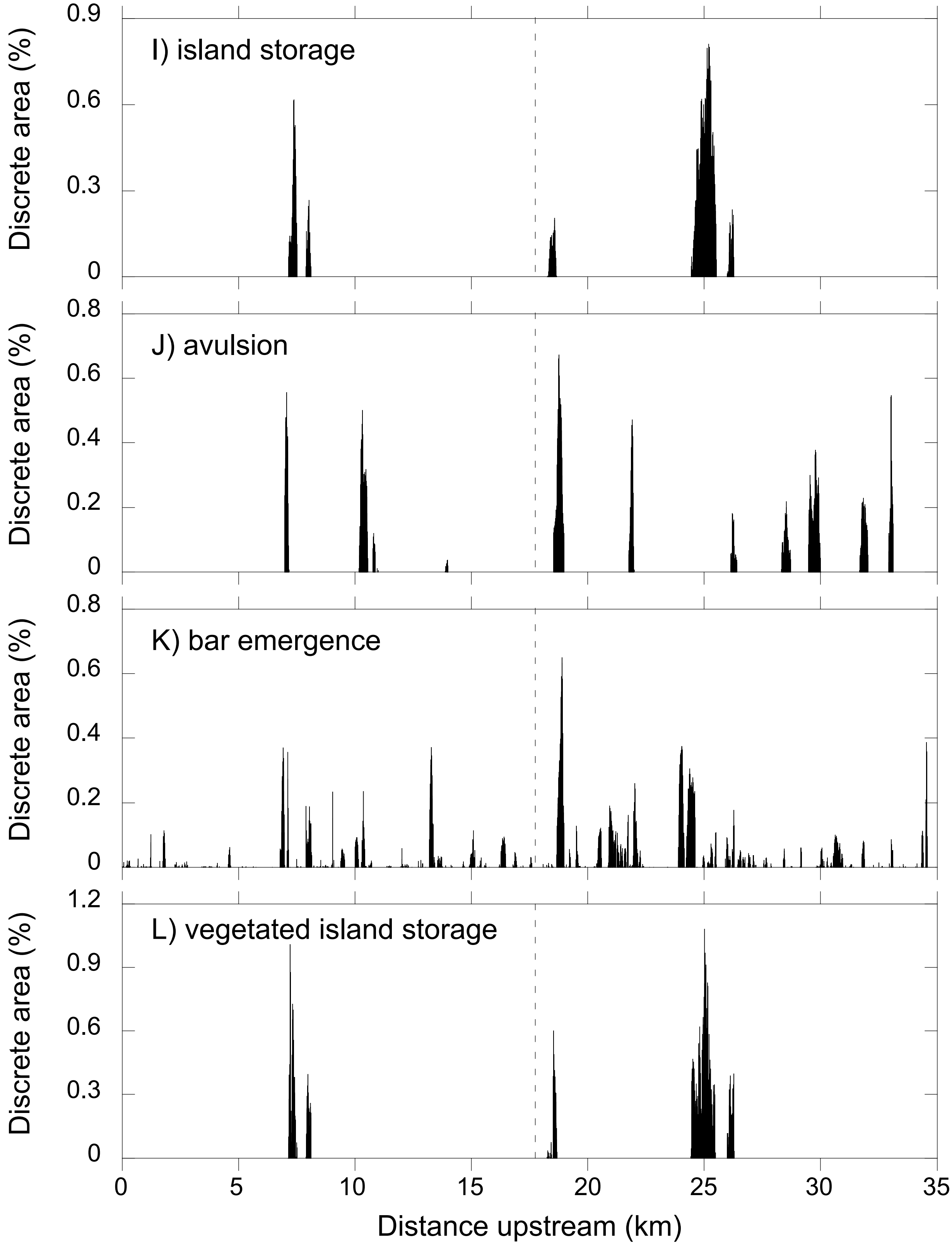
I) island storage
J) avulsion
K) bar emergence
L) vegetated island storage
Discrete area (%)
0
0.3
0.6
0.9
0.2
0.4
0.8
1.2
0
5
10
15
20
25
30
35
Distance upstream (km)

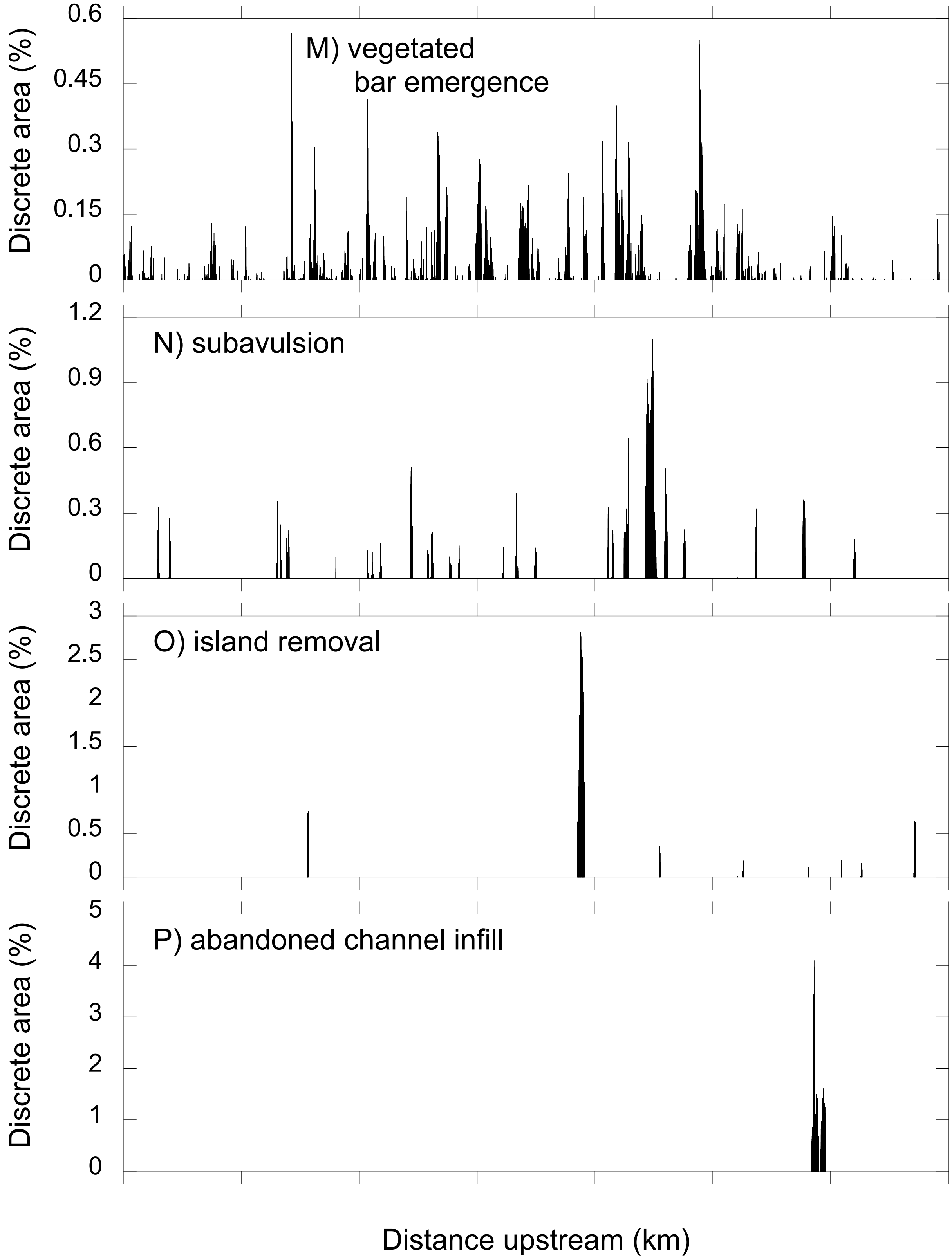

M) vegetated bar emergence
N) subavulsion
O) island removal
P) abandoned channel infill
Discrete area (%)
0
0.15
0.3
0.45
0.6
0.9
1.2
0.5
1
1.5
2
2.5
3
4
5
Distance upstream (km)

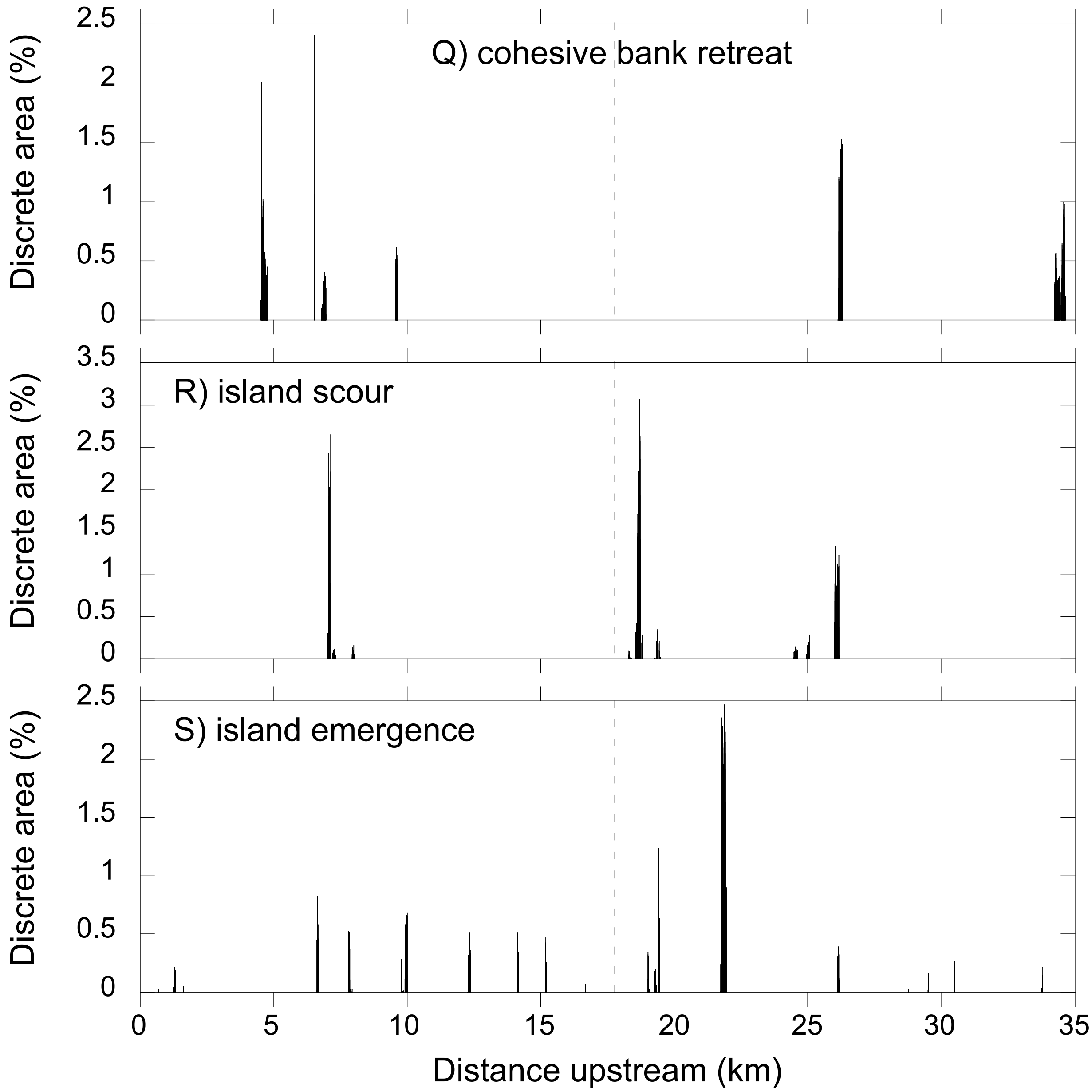
Q) cohesive bank retreat
R) island scour
S) island emergence
Discrete area (%)
Distance upstream (km)
0
5
10
15
20
25
30
35
0
0.5
1
1.5
2
2.5
3
3.5